Differential effect of silver nanoparticles on the microbiome of adult and developing planaria

DOI: doi.org/10.1016/j.aquatox.2020.105672
Handle: http://hdl.handle.net/1942/33314

Differential effect of silver nanoparticles on the microbiome of adult and developing planaria

Karolien Bijnens[a], Sofie Thijs[b], Nathalie Leynen[a], Vincent Stevens[b], Breanne McAmmond[c], Jonathan Van Hamme[c], Jaco Vangronsveld[b,d], Tom Artois[a], Karen Smeets[a]

[a]Centre for Environmental Sciences, Zoology, Biodiversity and Toxicology, Hasselt University, Hasselt, Belgium

[b]Centre for Environmental Sciences, Environmental Biology, Hasselt University, Hasselt, Belgium

[c]Department of Biological Sciences, Thompson Rivers University, Kamloops, British Columbia, Canada

[d]Department of Plant Physiology, Faculty of Biology and Biotechnology, Maria Skłodowska-Curie University, Lublin, Poland

Corresponding author:

Karen Smeets, karen.smeets@uhasselt.be

ORCID:

Karolien Bijnens, 0000-0001-7259-3464

Sofie Thijs, 0000-0002-2931-9619

Nathalie Leynen, 0000-0003-0534-8770

Vincent Stevens, 0000-0002-3725-1597

Breanne McAmmond, 0000-0001-5370-6152

Jonathan Van Hamme, 0000-0001-9471-7616

Jaco Vangronsveld, 0000-0003-4423-8363

Tom Artois, 0000-0002-2491-7273

Karen Smeets, 0000-0001-9673-8824

Abstract

Silver nanoparticles (AgNPs) are widely incorporated in household, consumer and medical products. Their unintentional release via wastewaters raises concerns on their environmental impact, particularly for aquatic organisms and their associated bacterial communities. It is known that the microbiome plays an important role in its host's health and physiology, *e.g.* by producing essential nutrients and providing protection against pathogens. A thorough understanding of the effects of AgNPs on bacterial communities and on their interactions with the host is crucial to fully assess AgNP toxicity on aquatic organisms. Our results indicate that the microbiome of the invertebrate *Schmidtea mediterranea*, a freshwater planarian, is affected by AgNP exposure at the tested 10 µg/ml concentration. Using targeted amplification of the bacterial 16S rRNA gene V3–V4 region, two independent experiments on the microbiomes of adult worms revealed a consistent decrease in Betaproteobacteriales after AgNP exposure, mainly attributed to a decrease in *Curvibacter* and *Undibacterium*. Although developing tissues and organisms are known to be more sensitive to toxic compounds, three independent experiments in regenerating worms showed a less pronounced effect of AgNP exposure on the microbiome, possibly because underlying bacterial community changes during development mask the AgNP induced effect. The presence of a polyvinyl-pyrrolidone (PVP) coating did not significantly alter the outcome of the experiments compared to those with uncoated particles. The observed variation between the different experiments underlines the highly variable nature of microbiomes and emphasises the need to repeat microbiome experiments, within and between physiological states of the animal.

Keywords

Silver nanoparticles, Planarians, Microbiome, Regeneration and development, Toxicity

1. Introduction

Silver nanoparticles (AgNPs) are one of the most important and widely used nanomaterials in many everyday household, medical and consumer items (Vance et al. 2015). Worldwide, about 135–420 tons of AgNPs are produced per year (Pulit-Prociak and Banach 2016) and it is estimated to grow to as much as 800 tons per year by 2025 (Porter and Youtie 2009). Due to their small size, AgNPs have a large surface to volume ratio, which gives them unique physicochemical, antimicrobial and anti-inflammatory properties (McGillicuddy et al. 2017). However, AgNP production, use, and waste disposal results in AgNPs release into the environment through wastewater, leading to adverse effects to ecosystems and inhabiting (aquatic) organisms (Gottschalk et al. 2009). Their physicochemical properties and antimicrobial activity raise the concern that AgNPs will not only have a toxic effect on the organisms themselves, but also on the associated microbiome.

Knowledge about the impact of AgNPs on bacterial communities is scant and, therefore, a detailed understanding on bacterial communities and their behaviour is crucial to fully assess AgNP toxicity in aquatic organisms and ecosystems. Current evidence suggests that both the nanoparticle itself, and the released silver ions (Ag^+) cause toxicity, although the underlying mechanisms are yet to be fully elucidated (Pulit-Prociak and Banach 2016; Tang and Zheng 2018). Several microbiome studies on AgNP toxicity do not take community dynamics into account as they only study a single bacterial species and/or do not consider different physiological conditions of the host (Liao et al. 2019; van den Brule et al. 2016). In addition, many microbiome studies base their conclusion on single experiments and do not consider individual variation (Dahan et al. 2018; Lekamge et al. 2018). Both information on individual variation and community dynamics are crucial to fully assess AgNP toxicity and to serve as a base for the establishment of effective governmental regulations and measures.

This contribution investigates the effects of AgNPs on the microbiome of the freshwater planarian *Schmidtea mediterranea*, Platyhelminthes. Almost each animal interacts with micro-organisms, at least during parts of its life (Hammer et al. 2019). We refer to the planarian-associated bacteria as ‘microbiome’, although it is still unclear if these bacteria are fixed or transient and which functional implications they have for the host. We do know that a pathogenic shift in the microbiome of planaria impedes tissue regeneration (Arnold et al. 2016), but the exact role of the microbiome remains to be elucidated. Since planarians live in the lowest water layer (benthic area), glide over surfaces using their motile cilia (Rompolas et al. 2009), and come directly in contact with sedimented AgNPs, they constitute

a highly representative model to study the effects of AgNPs on aquatic organisms. Although known as a classical regeneration model, *S. mediterranea* is also commonly used in toxicological research and risk assessment assays (Hagstrom et al. 2015; Stevens et al. 2017). Apart from their low maintenance effort and cost, the growing set of molecular tools and availability of planarian genome and transcriptome databases allows studying (stem) cell responses *in vivo* (Wu and Li 2018). Previously, planarians have already been used to assess nanoparticle toxicity and biocompatibility. For example, AgNP toxicity was first studied in *Girardia tigrina* (Kustov et al. 2014) and later in *S. mediterranea* (Leynen et al. 2019). In addition, the effects on stem cells and tissue regeneration of other nanomaterials including boron nitrate nanotubes (Salvetti et al. 2015) and cerium oxide nanoparticles (Salvetti et al. 2020) were investigated using *Dugesia japonica*. Planaria have a unique regenerative capacity: following injury, pluripotent stem cells (called neoblasts) are triggered to divide, migrate and differentiate to fully restore lost tissues, including a central nervous system, in approximately 10 days (Aboobaker 2011; Gentile et al. 2011; Zhu and Pearson 2016). Developing tissues are often more sensitive to toxic exposures (Falck et al. 2015; Neal-Kluever et al. 2014). Therefore, and because microbiomes are known to continuously change during the development of their host (Dirksen et al. 2016; Longo et al. 2015; Stephens et al. 2016), several stages of the regeneration process were included in this study.

To our knowledge, this is the first study addressing the effects of AgNPs on the microbiome of *S. mediterranea*, in adult worms as well as in developing tissues of regenerating worms. In a controlled laboratory environment, we evaluate two types of AgNPs: uncoated ones (NC-AgNPs) and polyvinyl-pyrrolidone-coated (PVP-AgNPs) ones, at a concentration of 10 µg/ml that is also found in polluted waters (Syafiuddin et al. 2018). PVP-AgNPs are supposed to be less toxic since PVP prevents ion leaching (Nymark et al. 2013), although some studies suggest that decreased agglomeration capacity results in increased toxicity (Leynen et al. 2019). Due to their antibacterial properties, we hypothesised that AgNPs might influence the microbiomes of adult and regenerating worms. We characterised the microbiome of *S. mediterranea* and, in contrast to other microbiome studies that base their conclusions on a single experiment (Dahan et al. 2018), included independent experiments taking variation factors such as time and season into account, allowing us to find fixed patterns in bacterial community shifts following AgNP exposure. We show that the planarian microbiome is variable and that AgNPs impact the microbiomes of both adults and regenerating worms. The observed effect was more pronounced in the microbiomes of adult worms, as bacterial community dynamics during the different developmental

stages possibly mask the AgNP effect. Our findings have important implications for toxicity studies, since an imbalance or disturbance of an organism's (commensal) microbiome might have far-reaching implications on host health and development.

2. Materials and methods

2.1. Planarian cultivation

An asexual strain of the planarian *S. mediterranea* was cultivated in freshwater medium consisting of 1.6 mM NaCl, 1 mM $CaCl_2$, 1 mM $MgSO_4$, 0.1 mM $MgCl_2$, 0.1 mM KCl and 1.2 mM $NaHCO_3$ in milliQ water (Pirotte et al. 2015). The worms were fed once a week with veal liver and kept in the dark at a constant temperature of 20° C. Worms of similar sizes (approximately 4–6 mm) were selected for experiments and starved seven days before exposure to AgNPs. In case developing worms were studied, the worms were cut transversally anterior to the pharynx to obtain a regenerating head and tail part just before exposure.

2.2. AgNP characterization, exposure and sampling

To assess the effect of AgNPs on the microbiome of *S. mediterranea,* we exposed the worms to AgNP-containing freshwater media. Two types of silver nanoparticles were used: uncoated (NC-AgNP) and polyvinyl-pyrrolidone-coated (PVP-AgNPs), both purchased from US Research Nanomaterials Inc (Houston, USA), both with nominal size of 20 nm. Stock dispersions (5 mg/ml) of NC-AgNP and PVP-AgNP were prepared in milliQ water as described by Leynen et al. (2019) and further diluted to a final concentration of 10 µg/ml in freshwater medium, the threshold known to induce sublethal adverse effects in *S. mediterranea* (Leynen et al. 2019). In addition, this concentration is found in polluted waters (Syafiuddin et al. 2018) and in the range of daily human intake (Vila et al. 2018; Wijnhoven et al. 2009). The AgNPs were characterized as described previously: the average diameter and structure of the AgNPs were studied with transmission electron microscopy (TEM, Philips EM 208 S) and the intensity-based hydrodynamic diameter (d_H), the zeta potential (z) and the dispersity index (D) of the exposure media were measured via dynamic light scattering (DLS, 80Plus Bi-MAS/ZetaPALS, Brookhaven Instruments Corporation, USA) (Leynen et al. 2019).

To evaluate replicability in time and better assess the robustness of the findings, we performed two independent experiments for adult worms (*Adult-1*, *Adult-2*), and three independent experiments for regenerating worms (*Dev-1*, *Dev-2*, *Dev-3*). We compared (1) the effects of AgNPs on the microbiomes

of adult and regenerating worms and (2) the effects of non-coated and PVP-coated AgNPs. By combining different experimental set-ups, we were able to address several in-depth research questions, simultaneously assessing variability of the results. An overview of the experimental set-up is presented in Fig. 1A, B. For the adult worms, 20 worms were individually exposed for seven days to 1 ml AgNP-containing media in sterile 24-well plates, divided over two independent experiments. In the *Adult-1* experiment, the microbiomes of 12 adult animals (*S. mediterranea*), four individuals per condition (non-exposed, NC-AgNP- and PVP-AgNP-exposed), were characterized (Fig. 1A). For each condition, at least one medium sample was included, resulting in 5–6 samples per condition. A second 7-day exposure experiment was performed independently (*Adult-2*), and included 4 non-exposed adult worms and 4 NC-AgNP-exposed adult worms. For the regenerating worms, we analysed the microbiomes of 2 × 45 regenerating head and tail fragments, divided over three independent experiments. Based on previous research (Leynen et al. 2019), the worms were allowed to regenerate for 3, 7 and 14 days, corresponding to an early, late and complete developmental stage. Since Leynen et al. (2019) found that a PVP-coating significantly altered tissue toxicity, experiments on the microbiomes of regenerating animals were mainly focussed on the effects of PVP-AgNPs. In *Dev-1* and *Dev-2*, three individual head and tail fragments were analysed per time-point per exposure group, while five head or tail fragments per exposure group were analysed in *Dev-3* (Fig. 1B). The AgNP-containing media were refreshed every 2–3 days. Before destructive sampling, individual tissue pieces were rinsed three times with sterile medium and then snap frozen in liquid nitrogen, stored at -74° C and processed further within two months.

2.3. DNA extraction

To obtain sufficient DNA from the low biomass samples, we used an optimised phenol-chloroform DNA extraction protocol, as explained in detail in the Supplemental materials and methods (Supplementary material S4). DNA samples were stored at -20° C. For each condition, at least one medium sample was included in the DNA-extractions, and a DNA-extraction blank.

2.4. Illumina library preparation and sequencing

Samples from experiment *Adult-1*, *Dev-1* and *Dev-2* were sequenced using Illumina technology, while samples from *Adult-2* and *Dev-3* were prepared for the Ion Torrent platform. In both cases, the planarian microbiome was characterised using gene amplification with primers targeting the 16S rRNA V3–V4 region, and platform-specific adaptors and barcodes as explained in the Supplemental material and

methods (Supplementary material S4). The quality checked 4 nM amplicon pool was sequenced using a MiSeq Reagent Kit v3 (600 cycle) (MS-102-3003) and PhiX Control v3 (FC-110-3001) on a MiSeq sequencing system (Hasselt University, Belgium), following the manufacturer's protocol.

2.5. Ion Torrent library preparation and sequencing

The library preparation for Ion Torrent sequencing consisted of a nested primer approach using 341F (5′-TAC GGG AGG CAG CAG-3′) and 806R (5′-GGA CTA CVS GGG TAT CTA AT-3') primers in the first round, and sequencing adaptor (underlined, underlined and bold) Ion Xpress barcoded (bold) 341F (5′-CCA TCT CAT CCC TGC GTG TCT CCG ACT CAG **CTA AGG TAA CGA T**TA CGG GAG GCA GCA G-3') with P1 (underlined) adapted 806R (5′-CCA CTA CGC CTC CGC TTT CCT CTC TAT GGG CAG TCG GTG ATG AC TAC VSG GGT ATC TAA T-3') primers in the second round. The PCR mastermix composition and PCR run conditions are described in the Supplementary materials and methods (Supplementary material S4). The equimolar barcoded samples were pooled prior to sequencing on a Ion S5 XL (Life Technologies Inc., Carlsbad, CA) running Torrent Suite 5.10.0, the library dilution factor was determined using an Ion Library Quantitation Kit and a QuantStudio 3 system. An Ion 520 & Ion 530 Kit-Chef on an Ion Chef system was used to prepare DNA for sequencing, and sequencing was performed on an Ion 530 chip using 400 bp chemistry.

2.6. Bioinformatics processing of the 16S rRNA sequence data

The generated FASTQ files were analysed in RStudio 1.2.1335, R version 3.5.3 (R Core Team, 2019) using the DADA2 (version 1.10.1) microbiome pipeline, which infers exact amplicon sequence variants (ASVs) from raw sequencing data (Callahan et al. 2016). For Illumina paired-end reads, the sequences were filtered and trimmed using the following parameters: trimLeft=c(17,21), truncLen=c(290,280), maxN=0, maxEE=c(2,2), truncQ=2, rm.phix=TRUE. Error rates were inferred and the filtered reads were de-replicated and de-noised using the DADA2 default parameters. For Ion Torrent single-end reads, the DADA2 script was adapted with custom filtering and trimming parameters: trimLeft=22, truncLen=c(230), maxN=0, maxEE=c(2), truncQ=2, rm.phyx=FALSE. The dataset was denoised using DADA2. After merging paired reads (for Illumina only) and removal of chimeras, an ASV table was build and taxonomy assigned using IdTaxa (DECIPHER, version 2.10.2) (Murali et al. 2018) and the SILVA_SSU_r132_March2018.RData training set (Quast et al. 2013; Yilmaz et al. 2014). The resulting ASVs and taxonomy tables were combined with the metadata file into a physeq object (phyloseq, version 1.26.1) (McMurdie and Holmes 2013) and a tree was generated using rtree (ape, version 5.3) (Paradis

and Schliep 2019). Contaminants were removed from the dataset using the package Decontam (version 1.2.1) applying the prevalence method with a 0.5 threshold value (Davis et al. 2018). Organelle contaminants such as mitochondria and chloroplasts were removed.

2.7. Taxonomic and functional analyses

For downstream analyses subsets per experiment were made and further analysed in RStudio 1.2.1335, R version 3.5.3. Samples with low read depth (< 750) were removed, unless specified otherwise (Supplemental material S6). Taxonomic analyses were performed using the phyloseq package: bar charts and boxplots were constructed, alpha- and beta-diversity indices were calculated, and a differential abundance analyses using DESeq2 (version 1.22.2) was done, all explained in further detail in Supplemental materials and methods (Supplementary material S4).

To study the functional effect of a bacterial community shift after AgNP-exposure, we inferred bacterial genes from the 16S rRNA sequences and searched for associated discriminative reactions, enzymes and pathways between the microbiomes of non-exposed and AgNP-exposed worms. ASV tables containing relative abundances together with the corresponding sequences to the Piphillin server (Narayan et al. 2020), using BioCyc version 22.5 as reference database. The resulting output was analysed by the linear discriminant analysis effect size (LEfSE) algorithm (Segata et al. 2011), using a threshold LDA score ≥ 2 ($p < 0.05$) on the Galaxy platform (Afgan et al. 2018). The resulting discriminative BioCyc IDs (Caspi et al. 2016; Karp et al. 2019) were then matched to their respective metabolic pathways and enzymes and summarised in Supplementary material S3.

2.8. Data availability

The raw 16s rRNA gene sequencing data were submitted to the Short Read Archive of NCBI with project identifier PRJNA675880 and individual FASTQ sample IDs SAMN1679118 – SAMN16729262. Full metadata on the datasets, together with ASV and taxonomy tables can be found in Supplementary material S1 and S2.

3. Results

3.1. *AgNP characterization and uptake*

Since several factors including particle size, shape, surface charge and coating influence AgNP toxicity (Li et al. 2019), we characterized the AgNP-containing media by TEM and DLS. Both particle types were spherical in shape (Fig. 1C), with an average diameter of 35 nm and 33.5 nm for NC-AgNP and PVP-

AgNPs respectively (Fig. 1D), approximately 1.5 times the size indicated by the manufacturer. The hydrodynamic diameters were measured using DLS and depicted in Fig. 1E. The volume-based D5, D50 and D95 sizes correspond to the 5 %, 50 % and 95 % of particles under the mentioned hydrodynamic diameter, meaning that 5 % of the NC-AgNP particles was below the size of 64.2 nm, 50 % below 141.1 nm and 95 % below 327.7 nm. For PVP-AgNPs, 5 % of the particles were found to be less than 45.8 nm in size, 50 % less than 105.9 nm and 95 % less than 245.1 nm. The zeta-potential was -9.43 mV and -6.59 mV for NC-AgNPs and PVP-AgNPs, respectively, suggesting that PVP-AgNPs form a slightly less stable dispersion compared to NC-AgNPs. Polydispersity indices of approximately 0.3 indicated that both AgNP-containing media were moderately disperse, with PVP-AgNPs having a slightly higher index than NC-AgNPs, suggesting a slightly higher tendency to form aggregates. Previously, we also showed by single-particle ICP-MS a most frequent size of 37 nm for both types of AgNPs and a mean size of 110 ± 2 nm and 101 ± 1 nm for NC-AgNPs and PVP-AgNPs, respectively (Leynen et al. 2019). After 48h, the moment we refreshed the AgNP-containing media, four times greater sedimentation was observed in NC-AgNPs solutions in comparison to PVP-AgNPs. Leynen et al. (2019) also showed that the concentrations of NC-AgNPs and PVP-AgNPs in medium without worms were three to seven times higher compared to the medium containing worms. Using confocal imaging, Leynen et al. (2019) observed that both types of AgNPs were taken up intracellular in the worm (Fig. S1A) and that a fraction of the AgNPs appeared to accumulate in the planarian gut (Fig. S1B).

3.2. Adult planarians:

The exposed adult worms showed a dragging behaviour and occasionally immobility instead of their normal gliding motion. These behavioural changes were previously extensively described by Leynen et al (2019). Here we further analysed the microbiome and therefore identified the associated bacteria by sequencing. After processing and quality filtering of the resulting sequences, a total of 132 657 good quality (Q20) Illumina sequences were obtained in the *Adult-1* experiment (Fig. 1A), with an average number of sequences per sample of 7803 ranging from 994 to 14 748 sequences per sample (Table S1). The second independent experiment (Fig. 1A, *Adult-2*) yielded a total of 41 641 Ion Torrent Q20 sequences, with an average of 5205 sequences per sample, ranging from 411 to 34 459 per sample (Table S2).

3.3. Betaproteobacteriales dominate the microbiome of adult worms

To characterize the bacterial component of adult planarian microbiomes, the relative abundances (RA) of sequencing-derived operational taxonomic units were determined for all samples at the phylum, class, order, family and genus levels (Fig. 2, and Fig. S3, Fig. S2 for taxonomic relationships). In the *Adult-1* experiment, the relative composition of bacteria in non-exposed worms mainly consisted of representatives of the phyla Proteobacteria (50.8 %) and Bacteroidetes (47.3 %) (Fig. S3A), with the dominant classes being Gammaproteobacteria (48.9 %) and Bacteroidia (47.3 %) (Fig. S3B). Bacteria belonging to order Betaproteobacteriales (46.8 %) (Fig. 2A), family Burkholderiaceae (46.6 %) (Fig. S3C) and the genera *Curvibacter* (30.9 %) and *Undibacterium* (7.9 %) (Fig. 2B) comprised the largest part of the Proteobacteria. The largest section of Bacteroidetes was characterized by Chitinophagales (47.1 %) (family Chitinophagaceae). The phyla Acidobacteria, Actinobacteria, Armantimonadetes, Firmicutes and Planctomycetes were also present, although their relative abundance was less than 1 % averaged over all non-exposed worm samples. The two medium samples that came into contact with the non-exposed worms mainly contained Gammaproteobacteria (99.8 %) of the genus *Undibacterium* (94.8 %). The independent experiment *Adult-2* confirmed the dominance of Betaproteobacteriales (75.4 %) (Fig. 2C), although apart from *Curvibacter* (13.6 %), other genera were observed such as *Candidatus (Ca.) Symbiobacter* (29.7 %)*, Acidovorax* (16.3 %) and *Methylophilus* (3.3 %) (Fig. 2D).

3.4. AgNPs change the composition of the adult planarian microbiome by affecting Betaproteobacteriales

In both experiments AgNPs affected the phylum Proteobacteria. In the first experiment (*Adult-1*), the slight increase (not significant (ns)) in the relative abundance of Proteobacteria (approx. +13 % in RA for both AgNP types) in AgNP-exposed microbiomes was caused by a significant increase in Alphaproteobacteria (both +25 %, $p < 0.05$) and a simultaneous decrease in Gammaproteobacteria (both -13 %, $p < 0.05$) (Fig. S3B). The increase in Alphaproteobacteria was more noticeable in the first experiment, and was attributed to an increase in Rhizobiales (both +15 %, $p < 0.05$) (Fig. 2A), mainly attributed to ASV-207 (DESeq2, $p < 0.05$) (genus *Afipia,* both +1 %) (Fig. 3A, B, Table S5). The decrease in Gammaproteobacteria in *Adult-1* was due to significant decreases (DESeq2, $p < 0.05$) in ASV-1 (genus *Curvibacter*, NC -27 %, PVP: -30 %), ASV-7 and ASV-70 (genus *Undibacterium*, both -8 %), all three Betaproteobacteriales (NC: -24.5 %, PVP: -32 %, $p < 0.05$) (Fig. 3A, B, Table S5) in both exposed groups. Compared to the non-exposed group, ASV-33 (genus *Rhodoferax,* -0.6 %) was decreased in the NC-AgNP-exposed group (Fig. 3A), while ASV-16 (genus *Pseudomonas* (-0.5 %) of the order

Pseudomonadales) was decreased (DESeq2, $p < 0.05$) in the PVP-AgNP-exposed group (Fig. 2B). The decrease in Betaproteobacteriales (-55 %) after NC-AgNP exposure, attributed to ASVs corresponding to *Curvibacter* (-13.5 %) and *Undibacterium* (-6 %) was confirmed in the independent experiment *Adult-2* (Fig. 2C, Fig. 3C, Table S6). Some variation at genus level was observed, since several genera were detected that were not present in *Adult-1* (Fig. 2D), all from the family Burkholderiaceae (Fig. 3C, Table S6).

The relative abundances of Firmicutes (*Adult-1*: NC: +3 %, PVP: +1.5 %, $p < 0.05$, *Adult-2*: +17 %, ns) and Actinobacteria (*Adult-1*: NC: +23 %; PVP: +28 %, *Adult-2*: +22.5 %, $p < 0.05$) were increased compared to non-exposed worms in both experiments (Fig S3A, D). In the first experiment (*Adult-1*), the phylum Acidobacteria was also significantly increased (NC: +3.5 %, PVP: +4.5 %, $p < 0.05$) compared to non-exposed worms. A strong decrease in Bacteroidetes (both -45.5%, $p < 0.05$) was observed after AgNP exposure in experiment *Adult-1* (Fig. S3A), which was attributed to a strong decrease in the class Bacteroidia (both -45.5 %, $p < 0.05$) (Fig. S3B) and more specifically in the order Chitinophagales (both -46 %, $p < 0.01$) (Fig. 2A), as several ASVs of this order were found to be differentially decreased (DESeq2, $p < 0.05$) (Fig. 3A, B, Table S5). In experiment *Adult-2* a slight increase in Bacteroidetes (ns) (Fig. S3D) was observed in one AgNP-exposed sample. Compared to non-exposed samples, the phyla Gemmatimonadetes, Verrucomicrobia, Chlamydiae, Fusobacteria and Chloroflexi were additionally detected after NC- or PVP-AgNP exposure in *Adult-1 (< 1 %* RA*)*, but not in the *Adult-2* experiment.

Comparing PVP-AgNP-exposed worms to NC-AgNP-exposed worms in the *Adult-1* experiment, only ASV-104 (*Methylovirgula*) was found to be significantly more present (DESeq2, $p < 0.05$) in PVP-AgNP-exposed worms, suggesting a limited effect of the PVP-coating on the microbiome (Table S5). The medium sample of the NC-AgNP exposure group had a microbial composition similar to that of the NC-AgNP-exposed worms, although it should be noted that this observation is only based on one medium sample (Fig. 2A). In the two medium samples of the PVP-AgNP-exposed group *Variovorax* (48.2 % RA), *Sphingopyxis* (7.6 % RA) and *Dyella* (4.0 % RA) were detected (Fig. 2B).

3.5. Alpha-diversity is affected by AgNP exposure in adult animals, although not consistently

Regarding the bacterial community diversity within individual samples, an increased Simpson's (both adj-p = 0.043) and Shannon's diversity (both adj-p = 0.043) was observed in NC-AgNP and PVP-AgNP exposed worms of the Adult-1 experiment, compared to the non-exposed condition (Fig. 4A). The observed ASV count was not significantly different ($p = 0.106$). The observed ASV number reflects the

samples richness, Shannon's diversity is strongly influenced by richness and the occurrence of rare species, while Simpson's diversity puts more weight to evenness and dominant species. The results were not consistent, since in experiment *Adult-2*, NC-AgNP exposure lowered the observed ASV number ($p = 0.013$) and Shannon's diversity ($p = 0.034$) (Fig. 4B). This observation may possibly be explained by the low read numbers in the exposed samples (Table S2).

3.6. Beta-diversity is consistently altered by AgNP exposure in adult animals

Both experiments showed similar results when the dissimilarity in community composition was quantified between samples, and compared among the different conditions. The MDS plot based on the Bray-Curtis index of dissimilarity in experiment *Adult-1* showed a separation between non-exposed and AgNP-exposed microbiomes ($p = 0.005$, $R^2 = 0.465$), along with a primary and secondary axis explaining respectively 37.6 % and 14.9 % of the total variation (Fig. 4C). Pairwise comparison of non-exposed with NC-AgNP- (adj-$p = 0.044$, $R^2 = 0.459$) or PVP-AgNP-exposed microbiomes (adj-$p = 0.044$, $R^2 = 0.460$) suggested that both exposed groups differed from non-exposed worms, although not from each other (adj-$p = 0.678$, $R^2 = 0.123$). The effect of AgNPs was confirmed in experiment *Adult-2*: a significant separation between non-exposed and NC-AgNP-exposed microbiomes ($p = 0.030$, $R^2 = 0.280$) was observed, along with the primary and secondary axis explaining 31.0 % and 17.9 % of variance respectively (Fig. 4D). In both experiments, the distance between non-exposed worms was less than the distance between exposed adults, suggesting more dissimilarity between individual exposed animals.

3.7. The microbiome of AgNP-exposed adult worms is enriched in predicted fatty acid metabolism genes

In total, 12 inferred genes were significantly more present (LEfSE LDA ≥ 2.7, $p < 0.05$) in the microbiome of non-exposed adults compared to AgNP-exposed adults (Fig. S4A) and were associated with biosynthesis pathways, electron transfer and enzymes such as cyclase, oxidase, kinase and isomerase. In addition, 57 features were enriched in the microbiomes of AgNP-exposed adults compared to non-exposed worms (Fig. S4B), most of them linked to the fatty acid metabolism: 30 genes were involved in the biosynthesis of fatty acids, including initiation reactions and myristate, palmitate and stearate biosynthesis. Fifteen genes were linked to fatty acid degradation, including oleate β-oxidation. Other discriminative genes associated with biosynthesis were involved in NAD metabolism and secondary

metabolite production, while other degradation genes were linked to amino acid and acrylonitrile degradation. Five hits enriched in AgNPs included genes linked with cyclase, transposase, monooxygenase, glyoxalase and electron transfer activity.

3.8. Regenerating planarians:

The regenerative defects in exposed regenerating worms described by Leynen et al (2019) were confirmed in this study. Here we further investigated the effect of AgNP exposure on the microbiome of regenerating worms. In experiment *Dev-1*, a non-exposed head and tail sample (3 dpa) were excluded due to the low number of sequencing reads. After processing and quality filtering of the resulting Illumina generated sequences, a total of 311 180 good quality (Q20) sequences were acquired, with an average number of 9152 sequences per sample (ranging from 2292 to 19 386) (Table S3). Similar read numbers were obtained in the *Dev-2* experiment (Table S3). In *Dev-3*, after excluding four samples due to low read depth, a total of 631 169 Ion Torrent Q20 sequences were obtained, with an average number of sequences per sample of 24 276 ranging from 747 to 125 475 (Table S4).

3.9. The microbiome is dominated by Betaproteobacteriales in regenerating worms

In all three independent experiments (*Dev-1*, *Dev-2* and *Dev-3*) and over all time-points, Gammaproteobacteria (95.8 % RA averaged) (Fig. S2, Fig. S5) were most abundant in non-exposed fragments, due to a dominance of Betaproteobacteriales (92.6 %) (Fig. 5A, B, C), and more specific, Burkholderiaceae (80.9 %). In 3 dpa non-exposed head and tail fragments, *Curvibacter* (75.8 %) dominated the microbiome in all three experiments. Species of *Burkholderia* sensu lato (s.l.) (*Burkholderia-Caballeronia-Paraburkholderia*) were detected occasionally in head samples. In experiment *Dev-3*, several samples showed a more diverse microbiome than in the two other experiments. The 7 dpa non-exposed microbiomes in *Dev-1* and *Dev-2* appeared similar to each other at higher taxonomic levels, although they were more variable at the genus level: in non-exposed head fragments *Curvibacter* (71.5 %) was most abundant, while *Burkholderia* s.l. (50.9 %) dominated non-exposed tail fragments (Fig. 5A, B). At complete development, 14 dpa, both *Burkholderia* s.l. (29.9 %) and *Curvibacter* (41.1 %) dominated non-exposed fragments (*Dev-1*, Fig. 5A). The results suggested that in non-exposed worms, the microbial composition is dependent on developmental stage and fragment type (especially 7 dpa).

3.10. AgNPs differentially impact the microbiome of head and tail fragments during development

An overall comparison of non-exposed and AgNP-exposed fragments showed differences in bacterial composition, mainly at the genus level (Fig. 5) and between developmental stages (Fig. S5). All experiments showed that PVP-AgNPs had a limited effect on 3 dpa head and tail microbiomes (Fig. 5, Fig. S5, Table S7-S9). However, some tail microbiomes of *Dev-3* were more affected by AgNP exposure than heads. In tail fragments, ASV-167 (*Undibacterium*, approx. -0.5 %) was significantly decreased (DESeq2, $p < 0.05$) in both AgNP-exposed microbiomes, compared to non-exposed tails (Fig 5C, Fig. S5C, Table S9). In addition, ASV-125 (*Corynebacterium_1*, NC: -0.3 %, PVP: -0.2 %) was decreased (DESeq2, $p < 0.05$) in NC-AgNP-exposed tail microbiomes only. PVP coating had a limited effect, since only the relative abundance of ASV-125 (DESeq2, $p < 0.05$) (*Corynebacterium_1*, +0.2 %) was increased in PVP-AgNP-exposed tails compared to NC-AgNP-exposed tails, while ASV-15 (*Curvibacter*, -39.7 %) was significantly decreased (DESeq2, $p < 0.05$). After 7 days of development, the effect of AgNP exposure on head microbiomes was more pronounced in *Dev-2* compared to *Dev-1*, as illustrated by an increase in the presence of the genus *Burkholderia* s.l. (+41 %) (Fig. 5B), attributed to ASV-63 (DESeq2, $p < 0.05$) (Fig. 6C, Table S8). Also 7 dpa tail microbiomes, in correspondence with 3 dpa tails, were more affected by AgNPs than heads, since in *Dev-1* seven ASVs decreased (DESeq2, $p < 0.05$) in relative abundance (Fig. 6A, Table S7). In *Dev-2*, exposed tail microbiomes were dominated by *Curvibacter* (+79.5 %) (Fig. 5B), represented by a significant increase (DESeq2, $p < 0.05$) of ASV-19 and ASV-1, while *Burkholderia* s.l. (-48.8 %), ASV-2, was significantly lower (DESeq2, $p < 0.05$) than non-exposed tails (Fig. 6B, Table S8). Finally, 14 dpa (*Dev-1*), head and tail microbiomes were affected in a similar manner by PVP-AgNP exposure, since ASV-45 and ASV-82 (*Curvibacter,* -37.8 %) became less abundant (DESeq2, $p < 0.05$), while ASV-2 (DESeq2, $p < 0.05$) contributed to the increase of *Burkholderia* s.l. (+51.7 %) (Fig. 5A, Fig. 6B, Table S7).

3.11. Alpha-diversity depends on developmental stage and regenerating fragment

At the beginning of tissue regeneration, 3 dpa, AgNP exposure did not significantly alter alpha-diversity in neither head nor tail microbiomes in experiment *Dev-1* and *Dev-2* (Fig. 7A, B, Fig. S6). However, in *Dev-3*, NC-AgNP exposure lowered Simpson's ($p = 0.0149$) and Shannon's diversity ($p = 0.0191$) in heads, but not in tail microbiomes (Fig. 7C). After 7 days of regeneration, AgNP exposure had no effect on alpha-diversity in head-associated bacteria (Fig. 7A, B). Only in tail fragments of *Dev-2*, PVP-AgNP exposure resulted in lower observed ASV number ($p = 0.0192$), Simpson's ($p = 0.0167$) and Shannon's

diversity (p = 0.0087) (Fig. 7B, Fig. S6C, D). Finally, PVP-AgNP exposure decreased Simpson's (p = 0.0050) and Shannon's diversity (p = 0.00902) in 14 dpa heads, but not in tail microbiomes (Fig. 7A, Fig. S6B).

3.12. AgNP exposure has a limited effect on the beta-diversity of microbiomes of regenerating planaria

Based on the Bray-Curtis dissimilarity index, we observed a significant difference in beta-diversity between the microbiomes of non-exposed and PVP-AgNP exposed worms (R^2 = 0.101, p = 0.001) in experiment *Dev-1*, partly depending on the developmental stage (exposure × developmental stage: R^2 = 0.0887, p = 0.0170) (Fig. 8A). A significant difference between microbiomes of head and tail fragments (R^2 = 0.041, p = 0.0340) and between microbiomes of 3, 7 and 14 dpa (R^2 = 0.243, p = 0.001) fragments was also observed, together with an interaction between both (fragment × developmental stage: R^2 = 0.133, p = 0.001). Together, the two MDS axes explained 71.1 % of the variation. The effect of PVP-AgNP exposure on the microbiome was not consistent in all experiments, since in *Dev-2*, no difference in diversity based on exposure alone was observed, although again a significant difference between head and tail fragments was found (R^2 = 0.128, p = 0.004), partly explained by the interaction with exposure (fragment × exposure: R^2 = 0.127, p = 0.004) and developmental stage (fragment × developmental stage × exposure: R^2 = 0.237, p = 0.001) (Fig. 8B). The two axes of the MDS plot explained 73.9 % of the variation. In *Dev-3*, no difference in beta-diversity due to exposure alone was found, although head and tail microbiomes significantly differed from each other (R^2 = 0.0858, p = 0.0210), partly due to the interaction with exposure (fragment × exposure: R^2 = 0.188, p = 0.002) (Fig. 8C). Approximately 51 % of the variation was explained by both MDS axes.

3.13. The microbiome of AgNP-exposed regenerating worms harbours less fatty acid and lipid degradation functionality

A predictive functional analysis was performed using the predicted metagenomes for bacteria detected in regenerating worms. Significant (LEfSE, $p < 0.05$) discriminative features with an LDA score ≥ 2.3 were selected and in total 27 genes were found that were more present in the microbiomes of non-exposed worms compared to AgNP-exposed worms (Fig. S7). Two biosynthesis genes were involved in fatty acid and vitamin biosynthesis, while 12 genes were found to be involved in degradation, utilization and assimilation reactions, of which nine were related to fatty acid and lipid degradation,

including oleate β-oxidation. Three other genes were involved in alcohol, aromatic compound and carboxylate degradation. In addition, six genes encoding for transporters were enriched in none-exposed ones, including five sugar transporters and one peptide transporter.

4. Discussion

Silver nanoparticles (AgNPs) are a threat to aquatic life: adverse effects have been described for aquatic organisms such as *Danio rerio* (zebrafish), *Daphnia magna* (water flea), *Oryzias lapites* (Japanese medaka), *Pimephales promelas* (fathead minnow) and *Oncorhynchus mykiss* (rainbow trout) (Chae et al. 2009; Griffitt et al. 2009; Laban et al. 2010; Ma et al. 2018; Mackevica et al. 2015; Scown et al. 2010; van Aerle et al. 2013). Until now, it has been rarely investigated if and how AgNPs at realistic environmental concentrations affect the microbiome of aquatic organisms. We used *S. mediterranea* as a freshwater aquatic model organism that comes in close contact with sedimented AgNPs as it glides over surfaces. In a previous study, we observed the presence of AgNPs in planarian epidermal and gut tissues immediately after exposure (Leynen et al. 2019), making them ideal organisms to study the impact of these particles on worm microbiomes. Leynen et al. (2019) found that AgNPs induce behavioural changes in both adult and developing worms, as well as developmental defects in regenerating animals. Underlying DNA damage and decreased stem cell proliferation was thought to cause the impaired tissue- and neuroregeneration. These toxicological findings are now expanded by the current microbiome study where bacterial composition shifts in *S. mediterranea* by AgNPs are described, resulting in valuable information to assess AgNP toxicity regarding both the planarian as its microbiome. As invertebrates are thought to rely even more on their so-called secondary genome for life-sustaining functions than humans do (Petersen and Osvatic 2018), it is even more important to include microbial responses in (eco)toxicological studies.

Our data indicated Proteobacteria as the most abundant phylum in the planarian microbiome (Fig. S3A, Fig S5), which is consistent with an earlier report in *S. mediterranea* by Arnold et al. (2016) and is also reported in the gut of marine and freshwater fishes (Egerton et al. 2018; Liu et al. 2016), several soil invertebrates such as *Caenorhabditis elegans* (da Silva Correia et al. 2018; Zhang et al. 2017) and lab-cultured sea urchins (Hakim et al. 2015). Proteobacteria includes gram-negative pathogenic and nitrogen fixating bacteria, and makes up one of the largest and most versatile phyla, exhibiting an extreme metabolic diversity (Marín 2014). Our data strengthen the hypothesis that bacterial taxa are

shared across flatworms of the family Dugesiidae as we observed genera such as *Rhodoferax*, *Pedobacter*, *Chryseobacterium*, *Acidovorax*, *Pseudomonas* and *Enterobacter* that were also found in lab-cultured and wild-type *S. mediterranea* (Arnold et al. 2016) and in the close relative *Dugesia japonica* (Lee et al. 2018). Compared to regenerating worms (Fig. S5), the microbiomes of adult worms were more diverse and include Bacteroidetes, Actinobacteria and Firmicutes in higher relative abundances (Fig. S3). In humans, the adult gut microbiome is more diverse than the microbiome of infants (Radjabzadeh et al. 2020), although a decrease in diversity during aging is also reported (Deng et al. 2019). The latter was also observed in mice, as a decrease in microbial diversity with increasing age was reported (Langille et al. 2014). Future research focussing on the microbial diversity during the different stages of development will reveal the physiological implications for the planarian. During the different stages of tissue development, we observed changes in bacterial composition (Fig. 5, Fig. S5). Developmental stage-specific signatures have also been observed in the intestinal and skin microbiota of zebrafish, *C. elegans* and common coqui (Dirksen et al. 2016; Longo et al. 2015; Stephens et al. 2016).

Exposure to AgNPs affected the microbiome of both adult and regenerating worms, albeit to a lesser extent in the latter. In adults, AgNPs induced a difference in beta-diversity (Fig. 4C, D), while changes in alpha-diversity were not consistent across experiments (Fig. 4A, B), possibly because of low read depth for exposed samples in the *Adult-2* experiment. The relative abundance of AgNP-sensitive bacteria such as Proteobacteria and Bacteroidetes decreased in favour of Firmicutes, Actinobacteria and Acidobacteria (Fig. S3A, D). In literature, the AgNP-sensitivity of Gram-negative bacteria such as Proteobacteria and Bacteroidetes is explained by the presence of an external lipopolysaccharide layer situated external of a thin layer of peptidoglycan (Pulit-Prociak and Banach 2016; Shrivastava et al. 2007). Actinobacteria and Firmicutes as Gram-positive bacteria, on the other hand, appear to be more resistant to AgNPs due to their comparatively thicker cell wall and larger fraction of peptidoglycan (Tang and Zheng 2018). An increased Firmicutes/Bacteriodetes ratio due to AgNP exposure was also observed in mice guts (van den Brule et al. 2016) and larvae of *Drosophila* (Han et al. 2014). Some Acidobacteria are able to produce exopolysaccharides (EPS) that modify the size and zeta potential of AgNPs, causing agglomeration (Wang et al. 2016). In a previous study, we found AgNP agglomerates in the planarian gut (Fig. S1) (Leynen et al. 2019), which may partly be due to the presence of EPS-producing bacteria, or the mucus produced by the gut goblet cells. At the level of order, we observed a

consistent decrease of Gammaproteobacteria (Fig. S3B, E) after AgNP exposure in adults, attributed to a strong decrease in Betaproteobacteriales (Fig. 2A, C), and more specifically the family Burkholderiaceae (Fig. S3C, F). This diverse family of bacteria is found in soils, water and polluted environments (Coenye and Vandamme 2003), and includes animal and plant symbionts, as well as important pathogens (Denny 2006; Schaffer 2015; Takeshita and Kikuchi 2017). Despite some variation, the two independent experiments with adult worms showed consistent patterns after AgNP exposure. In both experiments the observed decrease in Burkholderiaceae was mainly attributed to ASVs corresponding to *Curvibacter* and *Undibacterium* (Fig. 2B, D, Fig. 3), suggesting AgNP sensitivity, but the exact molecular mechanisms remain unknown. From previous research, we know that strains of *Curvibacter* and *Undibacterium* were found in aquatic environments (Gülay et al. 2018) and that *Curvibacter* produces quorum sensing N-acetyl homoserine lactones that shape the microbial community and thereby promote the ability to colonize the epidermis of *Hydra vulgaris* (Pietschke et al. 2017). It is possible that a decrease in *Curvibacter* leads to a decrease in associated quorum sensing molecules, that in its turn leads to secondary AgNP-indirect effects on the bacterial community, although this should be further investigated.

The predictive functional analyses indicated that the bacteria of AgNP-exposed adult planarians are enriched in genes related to fatty acid metabolism (Fig. S4). Given that AgNPs are linked with oxidative stress and are able to damage membranes (Li et al. 2019), we hypothesise that bacteria efficient in degrading damaged membranes and synthesizing new fatty acids to rebuild the membranes are more likely to tolerate AgNP exposure. It is, however, also possible that the differences in functionality are a direct reflection of the altered bacterial composition after AgNP exposure. Future meta-transcriptomic research on bacteria and *S. mediterranea* is crucial to further elucidate the interactions between planaria and their microbiomes and how AgNPs affect both, ultimately leading to a better risk assessment on AgNP toxicity. For adult individuals of *S. mediterranea*, Leynen et al. (2019) already found that 15 µg/ml AgNP exposure resulted in behavioural changes of the planarian, which was confirmed in this study. At higher concentrations (50 µg/ml), exposure resulted in typical screw-like movements and side-laying behaviour, suggesting neurological toxicity.

Compared to adults, developing organisms and tissues are often more susceptible to compound and particle exposures (Falck et al. 2015; Neal-Kluever et al. 2014). We previously found that 15 µg/ml AgNP exposure results in impaired tissue- and neuroregeneration in planarians, related to an altered stem cell

cycle and that the PVP coating enhanced AgNP toxicity (Leynen et al. 2019). Although interferences with the microbiome were linked to planarian regeneration in other studies (Arnold et al. 2016; Lee et al. 2018), our data did not show a strong impact of AgNPs in regenerating animals. We observed different responses in head and tail fragments, and at different developmental stages (Fig. 5, Fig. 6). Non-exposed head and tail fragments showed a different microbial composition 7 and 14 dpa, suggesting that apart from developmental stage-specific variations, tissue-specific variations were present. These findings need to be validated and further studied in-depth to fully understand the underlying bacterial changes during development. During regeneration, the effect of AgNPs was limited in the early stages (3 dpa). At 7 dpa the microbiome of tails was more affected than that of heads, especially *Burkholderia* s.l, as illustrated by a decrease in richness and evenness (Fig. 7, Fig. S6). At the end of the regeneration process (14 dpa) the bacterial communities in fully grown heads and tails showed similar patterns, characterized by an decrease in *Curvibacter* in favour of *Burkholderia* s.l. (family Burkholderiaceae). Little is known about the sensitivity of both genera to AgNPs, but we hypothesise that due to the decrease of the sensitive *Curvibacter* (as here demonstrated in adult worms), *Burkholderia* s.l. experiences less competition and is able to expand. This is further enhanced by microbial changes during development as illustrated by the increase over time of *Burkholderia* s.l. in non-exposed microbiomes. *Burkholderia* s.l. is a large and complex group, containing pathogenic, symbiotic and non-symbiotic strains from a very wide range of environmental and clinical habitats (Estrada-de Los Santos et al. 2018). To discriminate between the primary environmental species of *Paraburkholderia* and pathogenic species of *Burkholderia*, species level information is necessary. Future research that focusses on elucidating the dynamics between the members of the family Burkholderiaceae and understanding their interaction with planarians is necessary to fully interpret our data. Our functional analyses showed less discriminative genes (Fig. S7) compared to adults, confirming that AgNPs had a lower impact on developing microbiomes. We relate this latter to concurring microbiome changes during development that possibly masked the AgNP effect. A detailed study at the transcriptome level is needed to further elucidate the dynamics between *S. mediterranea* and its microbiome and the impact of AgNPs on both.

In literature, reports about the effects of AgNPs on the microbiome are not always consistent. This can be explained by the functionally and metabolically diverse nature of phyla: at the species or strain level it is well possible that different taxa of the same higher taxon behave completely differently, and hence

future studies should focus more on the lowest taxonomic level possible. Apart from taxonomic diversity, inconsistent results can also be explained by variation in the characteristics of the studied AgNPs (particle size, shape, surface coating) and actual exposure concentrations (Li et al. 2019). Positively charged AgNPs show a higher effectiveness against prokaryotes, followed by neutral, and, then negatively charged AgNPs (Abbaszadegan et al. 2015). Spherical AgNPs elicit higher antimicrobial effects than other shapes (Li et al. 2019) and smaller particles are able to enter the bacteria and perform their toxic effect by the release of silver ions (< 10 nm), while larger particles tend to react with the cell wall and bacterial membrane, leading to disintegration (Nino-Martinez et al. 2019; Qing et al. 2018). These findings emphasise the importance of documenting all characteristics of the used AgNPs as done in this study (Fig. 1C, D, E). Keeping particle size, shape and exposure concentrations constant, we found a limited effect of the PVP surface coating compared to non-coated AgNPs on the microbiome of adult and regenerating planarians, although it should be noted that these conclusions were only based on one independent experiment per physiological state. In adult worms, the bacterial alpha- and beta-diversity was not affected by the presence of the coating (Fig. 4A, C) and only one ASV was significantly altered between NC-AgNP- and PVP-AgNP-exposed microbiomes, corresponding to *Methylovirgula* from the order Rhizobiales (Table S5). In regenerating worms, only 2 ASVs in tail fragments were differentially altered between both types of AgNPs (Table S9). To further link the behaviour of both AgNP types with cellular uptake and toxicological responses, an in-depth AgNP characterization at the cellular level - using TEM - is needed. We showed that NC-AgNPs form a slightly more stable dispersion compared to PVP-AgNPs, while PVP-AgNPs have a slightly higher tendency to form aggregates (Fig. 1E), possibly influencing AgNP uptake and cellular responses. When worms came into contact with the medium, a lower concentration of AgNPs was measured compared to the medium itself, which is probably related to sedimentation. We hypothesise that aggregate uptake via the pharynx in the gut might be stimulated due to the resemblance to food particles, and that aggregates may be trapped in the mucus and therefore be less available to penetrate deeper in individual worm and bacterial cells, in contrast to diffusion of non-aggregated AgNPs. AgNP uptake and *in situ* effects should be further studied, in particular focussing on the planarian gut and mucus as previous research showed the presence of AgNP-agglomerates (Leynen et al. 2019).

We acknowledge that this study has some limitations: as taxonomic information was available at genus level for most ASVs, more in-depth sequencing will be necessary to identify species prior to making

strict abundance measurements using quantitative PCR. As has been observed in other studies, low mass samples are challenging to sequence, making alpha-diversity analyses less reliable (Lemos et al. 2011). Due to the smaller datasets, we used DESeq2 (and its internal normalization to take library size and compositional bias into account) for increased sensitivity, although this may be associated with a higher false discovery rate (Weiss et al. 2017). Knowledge about the function of the different bacterial taxa in planarians is scarce and our study did not address this, but based on inferred metagenomes and available literature we were able to make hypotheses.

5. Conclusions

To summarize our results, AgNPs induced a shift in the microbial composition associated with *S. mediterranea*. The changes appeared more pronounced in adults compared to regenerating organisms, probably attributed to the underlying microbial changes that occur during development. By comparing datasets of multiple independent experiments, we were able to find recurring patterns in *Curvibacter*, *Undibacterium* and *Burkholderia* s.l. relative abundances after AgNP exposure. Future work will have to focus on the impact of these bacterial community shifts, ideally at the lowest taxonomic level, on planarian health and physiology, since this knowledge is necessary to fully assess the risks and adverse outcomes associated with AgNP exposure.

Funding information

This work was supported by the Research Foundation Flanders (FWO) (G.0B83.17N, N1522719 and 1522015N), the Bijzonder OnderzoeksFonds of Hasselt University (BOF16NI03) and the Hasselt University Methusalem project (08M03VGRJ). The research leading to results presented in this publication was carried out with infrastructure funded by The European Marine Biological Resource Centre (EMBRC) Belgium - FWO project GOH3817N. Bioinformatics analyses were made possible thanks to the Flemish Supercomputer Centre (VSC) infrastructure, supported by the FWO.

Acknowledgements

The authors thank Natascha Steffanie and Ria Vanderspikken for their skilful technical assistance.

References

Abbaszadegan A, Ghahramani Y, Gholami A, et al. (2015) The Effect of Charge at the Surface of Silver Nanoparticles on Antimicrobial Activity against Gram-Positive and Gram-Negative Bacteria: A Preliminary Study. Journal of Nanomaterials 2015:1-8 doi:10.1155/2015/720654

Aboobaker AA (2011) Planarian stem cells: a simple paradigm for regeneration. Trends Cell Biol 21(5):304-11 doi:10.1016/j.tcb.2011.01.005
Afgan E, Baker D, Batut B, et al. (2018) The Galaxy platform for accessible, reproducible and collaborative biomedical analyses: 2018 update. Nucleic Acids Res 46(W1):W537-W544 doi:10.1093/nar/gky379
Arnold CP, Merryman MS, Harris-Arnold A, et al. (2016) Pathogenic shifts in endogenous microbiota impede tissue regeneration via distinct activation of TAK1/MKK/p38. Elife 5:e16793 doi:10.7554/eLife.16793
Callahan BJ, McMurdie PJ, Rosen MJ, Han AW, Johnson AJ, Holmes SP (2016) DADA2: High-resolution sample inference from Illumina amplicon data. Nat Methods 13(7):581-3 doi:10.1038/nmeth.3869
Caspi R, Billington R, Ferrer L, et al. (2016) The MetaCyc database of metabolic pathways and enzymes and the BioCyc collection of pathway/genome databases. Nucleic Acids Res 44(D1):D471-80 doi:10.1093/nar/gkv1164
Chae YJ, Pham CH, Lee J, Bae E, Yi J, Gu MB (2009) Evaluation of the toxic impact of silver nanoparticles on Japanese medaka (Oryzias latipes). Aquat Toxicol 94(4):320-7 doi:10.1016/j.aquatox.2009.07.019
Coenye T, Vandamme P (2003) Diversity and significance of Burkholderia species occupying diverse ecological niches. Environ Microbiol 5(9):719-29 doi:10.1046/j.1462-2920.2003.00471.x
da Silva Correia D, Passos SR, Proença DN, Morais PV, Xavier GR, Correia MEF (2018) Microbial diversity associated to the intestinal tract of soil invertebrates. Applied Soil Ecology 131:38-46 doi:10.1016/j.apsoil.2018.07.009
Dahan D, Jude BA, Lamendella R, Keesing F, Perron GG (2018) Exposure to Arsenic Alters the Microbiome of Larval Zebrafish. Front Microbiol 9:1323 doi:10.3389/fmicb.2018.01323
Davis NM, Proctor DM, Holmes SP, Relman DA, Callahan BJ (2018) Simple statistical identification and removal of contaminant sequences in marker-gene and metagenomics data. Microbiome 6(1):226 doi:10.1186/s40168-018-0605-2
Deng F, Li Y, Zhao J (2019) The gut microbiome of healthy long-living people. Aging (Albany NY) 11(2):289-290 doi:10.18632/aging.101771
Denny T (2006) Plant pathogenic Ralstonia species. In: Gnanamanickam SS (ed) Plant-Associated Bacteria. Springer Netherlands, Dordrecht, p 573-644
Dirksen P, Marsh SA, Braker I, et al. (2016) The native microbiome of the nematode Caenorhabditis elegans: gateway to a new host-microbiome model. BMC Biol 14(1):38 doi:10.1186/s12915-016-0258-1
Egerton S, Culloty S, Whooley J, Stanton C, Ross RP (2018) The Gut Microbiota of Marine Fish. Front Microbiol 9(873):873 doi:10.3389/fmicb.2018.00873
Estrada-de Los Santos P, Palmer M, Chavez-Ramirez B, et al. (2018) Whole Genome Analyses Suggests that Burkholderia sensu lato Contains Two Additional Novel Genera (Mycetohabitans gen. nov., and Trinickia gen. nov.): Implications for the Evolution of Diazotrophy and Nodulation in the Burkholderiaceae. Genes (Basel) 9(8):389 doi:10.3390/genes9080389
Falck AJ, Mooney S, Kapoor SS, White KM, Bearer C, El Metwally D (2015) Developmental Exposure to Environmental Toxicants. Pediatr Clin North Am 62(5):1173-97 doi:10.1016/j.pcl.2015.05.005
Gentile L, Cebria F, Bartscherer K (2011) The planarian flatworm: an in vivo model for stem cell biology and nervous system regeneration. Dis Model Mech 4(1):12-9 doi:10.1242/dmm.006692
Gottschalk F, Sonderer T, Scholz RW, Nowack B (2009) Modeled environmental concentrations of engineered nanomaterials (TiO(2), ZnO, Ag, CNT, Fullerenes) for different regions. Environ Sci Technol 43(24):9216-22 doi:10.1021/es9015553
Griffitt RJ, Hyndman K, Denslow ND, Barber DS (2009) Comparison of molecular and histological changes in zebrafish gills exposed to metallic nanoparticles. Toxicol Sci 107(2):404-15 doi:10.1093/toxsci/kfn256

Gülay A, Çekiç Y, Musovic S, Albrechtsen H-J, Smets BF (2018) Diversity of Iron Oxidizers in Groundwater-Fed Rapid Sand Filters: Evidence of Fe(II)-Dependent Growth by Curvibacter and Undibacterium spp. Frontiers in Microbiology 9:2808
Hagstrom D, Cochet-Escartin O, Zhang S, Khuu C, Collins EM (2015) Freshwater Planarians as an Alternative Animal Model for Neurotoxicology. Toxicol Sci 147(1):270-85 doi:10.1093/toxsci/kfv129
Hakim JA, Koo H, Dennis LN, et al. (2015) An abundance of Epsilonproteobacteria revealed in the gut microbiome of the laboratory cultured sea urchin, Lytechinus variegatus. Front Microbiol 6:1047 doi:10.3389/fmicb.2015.01047
Hammer TJ, Sanders JG, Fierer N (2019) Not all animals need a microbiome. FEMS Microbiol Lett 366(10) doi:10.1093/femsle/fnz117
Han X, Geller B, Moniz K, Das P, Chippindale AK, Walker VK (2014) Monitoring the developmental impact of copper and silver nanoparticle exposure in Drosophila and their microbiomes. Sci Total Environ 487(1879-1026 (Electronic)):822-9
Karp PD, Billington R, Caspi R, et al. (2019) The BioCyc collection of microbial genomes and metabolic pathways. Brief Bioinform 20(4):1085-1093 doi:10.1093/bib/bbx085
Kustov L, Tiras K, Al-Abed S, Golovina N, Ananyan M (2014) Estimation of the toxicity of silver nanoparticles by using planarian flatworms. Altern Lab Anim 42(1):51-8 doi:10.1177/026119291404200108
Laban G, Nies LF, Turco RF, Bickham JW, Sepulveda MS (2010) The effects of silver nanoparticles on fathead minnow (Pimephales promelas) embryos. Ecotoxicology 19(1):185-95 doi:10.1007/s10646-009-0404-4
Langille MG, Meehan CJ, Koenig JE, et al. (2014) Microbial shifts in the aging mouse gut. Microbiome 2(1):50 doi:10.1186/s40168-014-0050-9
Lee FJ, Williams KB, Levin M, Wolfe BE (2018) The Bacterial Metabolite Indole Inhibits Regeneration of the Planarian Flatworm Dugesia japonica. iScience 10:135-148 doi:10.1016/j.isci.2018.11.021
Lekamge S, Miranda AF, Abraham A, et al. (2018) The Toxicity of Silver Nanoparticles (AgNPs) to Three Freshwater Invertebrates With Different Life Strategies: Hydra vulgaris, Daphnia carinata, and Paratya australiensis. Frontiers in Environmental Science 6:152
Lemos LN, Fulthorpe RR, Triplett EW, Roesch LF (2011) Rethinking microbial diversity analysis in the high throughput sequencing era. J Microbiol Methods 86(1):42-51 doi:10.1016/j.mimet.2011.03.014
Leynen N, Van Belleghem F, Wouters A, et al. (2019) In vivo Toxicity Assessment of Silver Nanoparticles in Homeostatic versus Regenerating Planarians. Nanotoxicology 13(4):476-491 doi:10.1080/17435390.2018.1553252
Li J, Tang M, Xue Y (2019) Review of the effects of silver nanoparticle exposure on gut bacteria. J Appl Toxicol 39(1):27-37 doi:10.1002/jat.3729
Liao S, Zhang Y, Pan X, et al. (2019) Antibacterial activity and mechanism of silver nanoparticles against multidrug-resistant Pseudomonas aeruginosa. Int J Nanomedicine 14:1469-1487 doi:10.2147/IJN.S191340
Liu H, Guo X, Gooneratne R, et al. (2016) The gut microbiome and degradation enzyme activity of wild freshwater fishes influenced by their trophic levels. Sci Rep 6(1):24340 doi:10.1038/srep24340
Longo AV, Savage AE, Hewson I, Zamudio KR (2015) Seasonal and ontogenetic variation of skin microbial communities and relationships to natural disease dynamics in declining amphibians. R Soc Open Sci 2(7):140377 doi:10.1098/rsos.140377
Ma Y, Song L, Lei Y, et al. (2018) Sex dependent effects of silver nanoparticles on the zebrafish gut microbiota. Environmental Science: Nano 5(3):740-751 doi:10.1039/c7en00740j
Mackevica A, Skjolding LM, Gergs A, Palmqvist A, Baun A (2015) Chronic toxicity of silver nanoparticles to Daphnia magna under different feeding conditions. Aquat Toxicol 161:10-6 doi:10.1016/j.aquatox.2015.01.023

Marín I (2014) Proteobacteria. In: Amils R, Gargaud M, Cernicharo Quintanilla J, et al. (eds) Encyclopedia of Astrobiology. Springer Berlin Heidelberg, Berlin, Heidelberg, p 1-2
McGillicuddy E, Murray I, Kavanagh S, et al. (2017) Silver nanoparticles in the environment: Sources, detection and ecotoxicology. Sci Total Environ 575(1879-1026 (Electronic)):231-246 doi:10.1016/j.scitotenv.2016.10.041
McMurdie PJ, Holmes S (2013) phyloseq: an R package for reproducible interactive analysis and graphics of microbiome census data. PLoS One 8(4):e61217 doi:10.1371/journal.pone.0061217
Murali A, Bhargava A, Wright ES (2018) IDTAXA: a novel approach for accurate taxonomic classification of microbiome sequences. Microbiome 6(1):140 doi:10.1186/s40168-018-0521-5
Narayan NR, Weinmaier T, Laserna-Mendieta EJ, et al. (2020) Piphillin predicts metagenomic composition and dynamics from DADA2-corrected 16S rDNA sequences. BMC Genomics 21(1):56 doi:10.1186/s12864-019-6427-1
Neal-Kluever A, Aungst J, Gu Y, et al. (2014) Infant toxicology: state of the science and considerations in evaluation of safety. Food Chem Toxicol 70:68-83 doi:10.1016/j.fct.2014.05.003
Nino-Martinez N, Salas Orozco MF, Martinez-Castanon GA, Torres Mendez F, Ruiz F (2019) Molecular Mechanisms of Bacterial Resistance to Metal and Metal Oxide Nanoparticles. Int J Mol Sci 20(11) doi:10.3390/ijms20112808
Nymark P, Catalan J, Suhonen S, et al. (2013) Genotoxicity of polyvinylpyrrolidone-coated silver nanoparticles in BEAS 2B cells. Toxicology 313(1):38-48 doi:10.1016/j.tox.2012.09.014
Paradis E, Schliep K (2019) ape 5.0: an environment for modern phylogenetics and evolutionary analyses in R. Bioinformatics 35(3):526-528 doi:10.1093/bioinformatics/bty633
Petersen JM, Osvatic J (2018) Microbiomes In Natura: Importance of Invertebrates in Understanding the Natural Variety of Animal-Microbe Interactions. mSystems 3(2):e00179-17 doi:10.1128/mSystems.00179-17
Pietschke C, Treitz C, Foret S, et al. (2017) Host modification of a bacterial quorum-sensing signal induces a phenotypic switch in bacterial symbionts. Proc Natl Acad Sci U S A 114(40):E8488-E8497 doi:10.1073/pnas.1706879114
Pirotte N, Stevens AS, Fraguas S, et al. (2015) Reactive Oxygen Species in Planarian Regeneration: An Upstream Necessity for Correct Patterning and Brain Formation. Oxid Med Cell Longev 2015:392476 doi:10.1155/2015/392476
Porter AL, Youtie J (2009) How interdisciplinary is nanotechnology? J Nanopart Res 11(5):1023-1041 doi:10.1007/s11051-009-9607-0
Pulit-Prociak J, Banach M (2016) Silver nanoparticles – a material of the future…? Open Chemistry 14(1):76-91 doi:10.1515/chem-2016-0005
Qing Y, Cheng L, Li R, et al. (2018) Potential antibacterial mechanism of silver nanoparticles and the optimization of orthopedic implants by advanced modification technologies. Int J Nanomedicine 13:3311-3327 doi:10.2147/IJN.S165125
Quast C, Pruesse E, Yilmaz P, et al. (2013) The SILVA ribosomal RNA gene database project: improved data processing and web-based tools. Nucleic Acids Res 41(Database issue):D590-6 doi:10.1093/nar/gks1219
Radjabzadeh D, Boer CG, Beth SA, et al. (2020) Diversity, compositional and functional differences between gut microbiota of children and adults. Sci Rep 10(1):1040 doi:10.1038/s41598-020-57734-z
Rompolas P, Patel-King RS, King SM (2009) Schmidtea mediterranea: a model system for analysis of motile cilia. Methods Cell Biol 93(0091-679X (Print)):81-98 doi:10.1016/S0091-679X(08)93004-1
Salvetti A, Gambino G, Rossi L, et al. (2020) Stem cell and tissue regeneration analysis in low-dose irradiated planarians treated with cerium oxide nanoparticles. Mater Sci Eng C Mater Biol Appl 115:111113 doi:10.1016/j.msec.2020.111113

Salvetti A, Rossi L, Iacopetti P, et al. (2015) In vivo biocompatibility of boron nitride nanotubes: effects on stem cell biology and tissue regeneration in planarians. Nanomedicine (London, England) 10(12):1911-22 doi:10.2217/nnm.15.46
Schaffer K (2015) Epidemiology of infection and current guidelines for infection prevention in cystic fibrosis patients. J Hosp Infect 89(4):309-13 doi:10.1016/j.jhin.2015.02.005
Scown TM, Santos EM, Johnston BD, et al. (2010) Effects of aqueous exposure to silver nanoparticles of different sizes in rainbow trout. Toxicol Sci 115(2):521-34 doi:10.1093/toxsci/kfq076
Segata N, Izard J, Waldron L, et al. (2011) Metagenomic biomarker discovery and explanation. Genome Biol 12(6):R60 doi:10.1186/gb-2011-12-6-r60
Shrivastava S, Bera T, Roy A, Singh G, Ramachandrarao P, Dash D (2007) Characterization of enhanced antibacterial effects of novel silver nanoparticles. Nanotechnology 18(22):225103 doi:10.1088/0957-4484/18/22/225103
Stephens WZ, Burns AR, Stagaman K, et al. (2016) The composition of the zebrafish intestinal microbial community varies across development. ISME J 10(3):644-54 doi:10.1038/ismej.2015.140
Stevens AS, Willems M, Plusquin M, et al. (2017) Stem cell proliferation patterns as an alternative for in vivo prediction and discrimination of carcinogenic compounds. Sci Rep 7:45616 doi:10.1038/srep45616
Syafiuddin A, Salmiati S, Hadibarata T, Kueh ABH, Salim MR, Zaini MAA (2018) Silver Nanoparticles in the Water Environment in Malaysia: Inspection, characterization, removal, modeling, and future perspective. Sci Rep 8(1):986 doi:10.1038/s41598-018-19375-1
Takeshita K, Kikuchi Y (2017) Riptortus pedestris and Burkholderia symbiont: an ideal model system for insect-microbe symbiotic associations. Res Microbiol 168(3):175-187 doi:10.1016/j.resmic.2016.11.005
Tang S, Zheng J (2018) Antibacterial Activity of Silver Nanoparticles: Structural Effects. Adv Healthc Mater 7(13):e1701503 doi:10.1002/adhm.201701503
van Aerle R, Lange A, Moorhouse A, et al. (2013) Molecular mechanisms of toxicity of silver nanoparticles in zebrafish embryos. Environ Sci Technol 47(14):8005-14 doi:10.1021/es401758d
van den Brule S, Ambroise J, Lecloux H, et al. (2016) Dietary silver nanoparticles can disturb the gut microbiota in mice. Part Fibre Toxicol 13(1):38 doi:10.1186/s12989-016-0149-1
Vance ME, Kuiken T, Vejerano EP, et al. (2015) Nanotechnology in the real world: Redeveloping the nanomaterial consumer products inventory. Beilstein J Nanotechnol 6:1769-80 doi:10.3762/bjnano.6.181
Vila L, Garcia-Rodriguez A, Cortes C, Marcos R, Hernandez A (2018) Assessing the effects of silver nanoparticles on monolayers of differentiated Caco-2 cells, as a model of intestinal barrier. Food Chem Toxicol 116(Pt B):1-10 doi:10.1016/j.fct.2018.04.008
Wang Q, Kang F, Gao Y, Mao X, Hu X (2016) Sequestration of nanoparticles by an EPS matrix reduces the particle-specific bactericidal activity. Sci Rep 6(1):21379 doi:10.1038/srep21379
Weiss S, Xu ZZ, Peddada S, et al. (2017) Normalization and microbial differential abundance strategies depend upon data characteristics. Microbiome 5(1):27 doi:10.1186/s40168-017-0237-y
Wijnhoven SWP, Peijnenburg WJGM, Herberts CA, et al. (2009) Nano-silver – a review of available data and knowledge gaps in human and environmental risk assessment. Nanotoxicology 3(2):109-138 doi:10.1080/17435390902725914
Wu JP, Li MH (2018) The use of freshwater planarians in environmental toxicology studies: Advantages and potential. Ecotoxicol Environ Saf 161:45-56 doi:10.1016/j.ecoenv.2018.05.057
Yilmaz P, Parfrey LW, Yarza P, et al. (2014) The SILVA and "All-species Living Tree Project (LTP)" taxonomic frameworks. Nucleic Acids Res 42(Database issue):D643-8 doi:10.1093/nar/gkt1209

Zhang F, Berg M, Dierking K, et al. (2017) Caenorhabditis elegans as a Model for Microbiome Research. Frontiers in Microbiology 8:485
Zhu SJ, Pearson BJ (2016) (Neo)blast from the past: new insights into planarian stem cell lineages. Curr Opin Genet Dev 40(1879-0380 (Electronic)):74-80

Figures

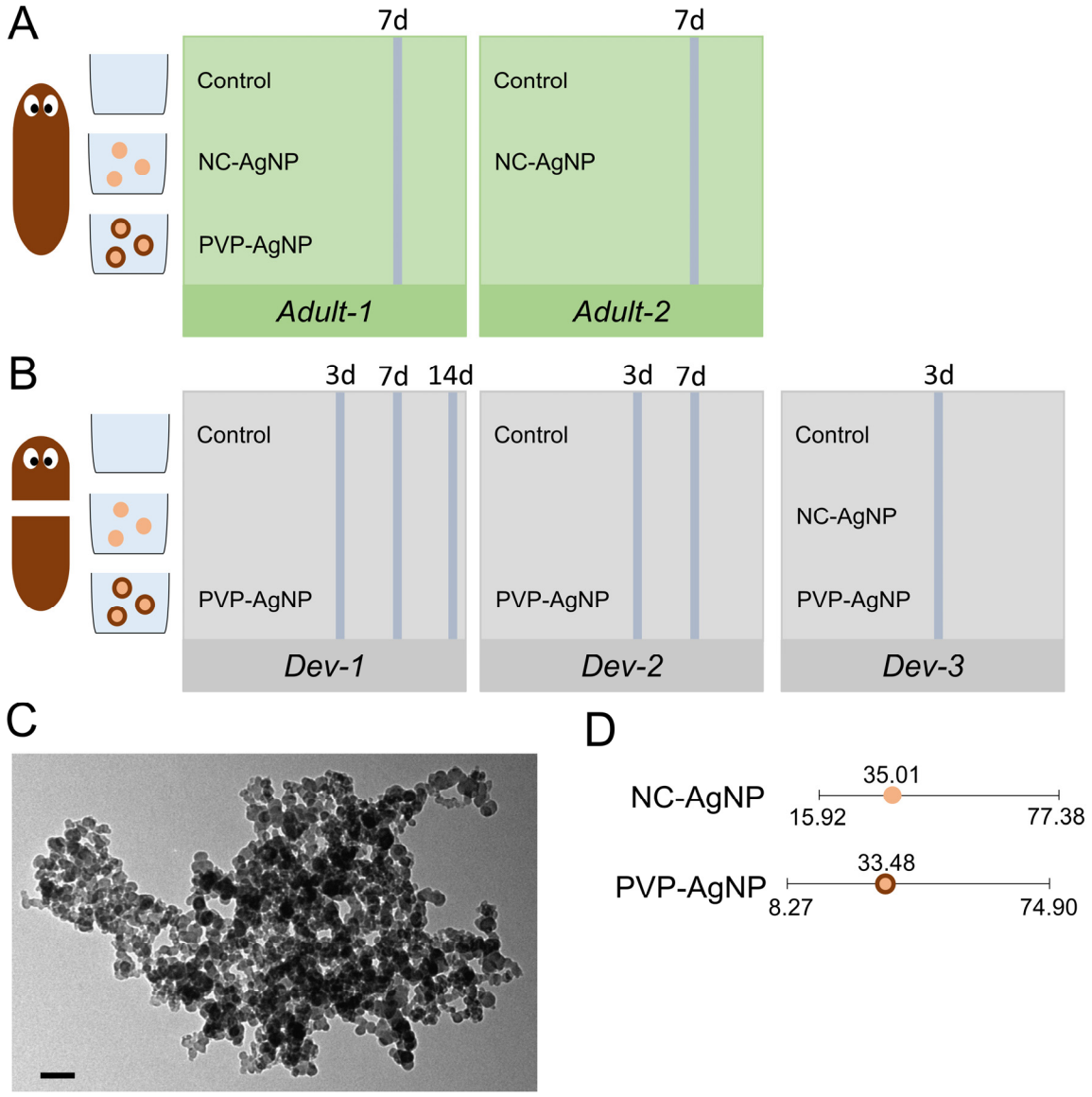

E

	Hydrodynamic diameter d_H (nm)			Zeta-potential (ζ)	Dispersity index (D)
	D5	D50	D95		
NC-AgNP	64.2	141.1	327.7	-9.43 mV	0.298
PVP-AgNP	45.8	105.9	245.1	-6.59 mV	0.317

Fig. 1 Experimental setup and nanoparticle characterization. **A** Experimental setup of adult worms: two independent experiments were performed, referred to as *Adult-1* and *Adult-2*. **B** Experimental setup of regenerating/developing worms: three independent experiments were performed, referred to as *Dev-1*, *Dev-2* and *Dev-3*. The microbiomes of *Adult-1*, *Dev-1* and *Dev-2* were sequenced by Illumina technology, the microbiomes of *Adult-2* and *Dev-3* using Ion Torrent technology. **C** Representative image of NC-AgNPs by TEM, scale representing 100 nm. **D** Average AgNP particle size (nm) with minimum and maximum sizes, measured by TEM (NC-AgNP n = 84 , PVP-AgNP n = 135). **E** The hydrodynamic diameters (d_H, nm), zeta-potentials (z) and dispersity index (D) by DLS. Volume-based D5, D50 and D95 sizes correspond to the 5 %, 50 % and 95 % of particles under the reported d_H. (NC-AgNP: non-coated silver nanoparticles, PVP-AgNP: polyvinylpyrrolidone-coated silver nanoparticles, d: days of exposure)

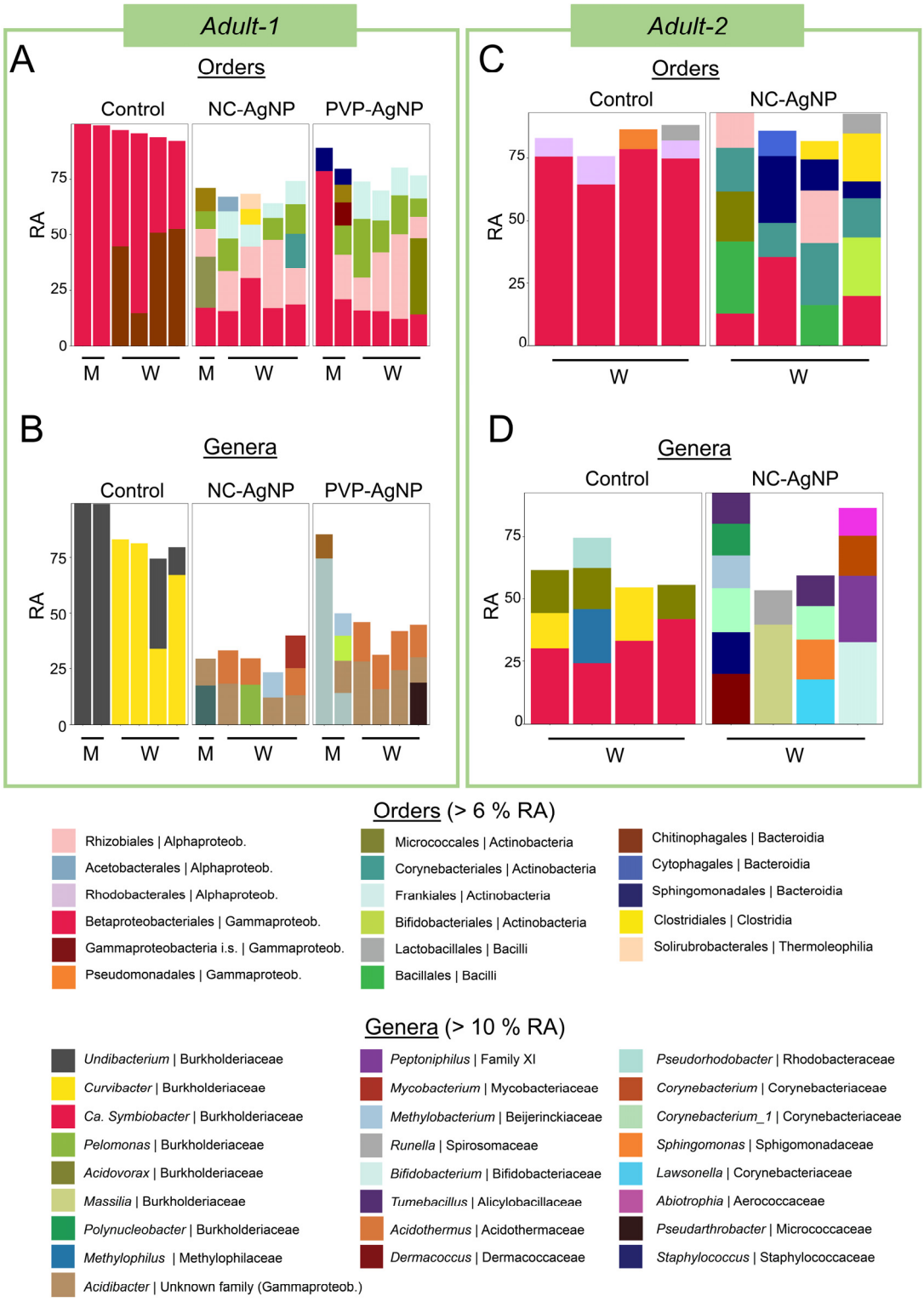

Fig. 2 Relative abundance (RA) of taxa in adult worms exposed for 7 days to AgNPs. **A** Bar charts representing the microbial composition of *Adult-1*, exposed to NC-AgNPs or PVP-AgNPs on order level classification, filtered to remove taxa below 6 % abundance. (Non-exposed n = 6, NC-AgNP n = 5, PVP-AgNP n = 6) **B** RA of the taxa in samples from the *Adult-1* experiment on genus level classification (> 10 % RA). **C** RA of the taxa in samples from *Adult-2*, on order level classification (> 6 % RA) (Non-exposed n = 4, NC-AgNP n = 4) **D** RA of the taxa in samples of *Adult-2* on genus level classification (> 10 RA). (The data in *Adult-1* and *Adult-2* represent two independent experiments. NC-AgNPs: non-coated silver nanoparticles, PVP-AgNPs: polyvinylpyrrolidone coated silver nanoparticles, RA: relative abundance, W: adult worms, M: exposure medium that came into contact with the worm, *Ca.: Candidatus*, i.s.: incertae sedis. At the right side of the pipe symbol (|), the corresponding higher taxon is indicated.)

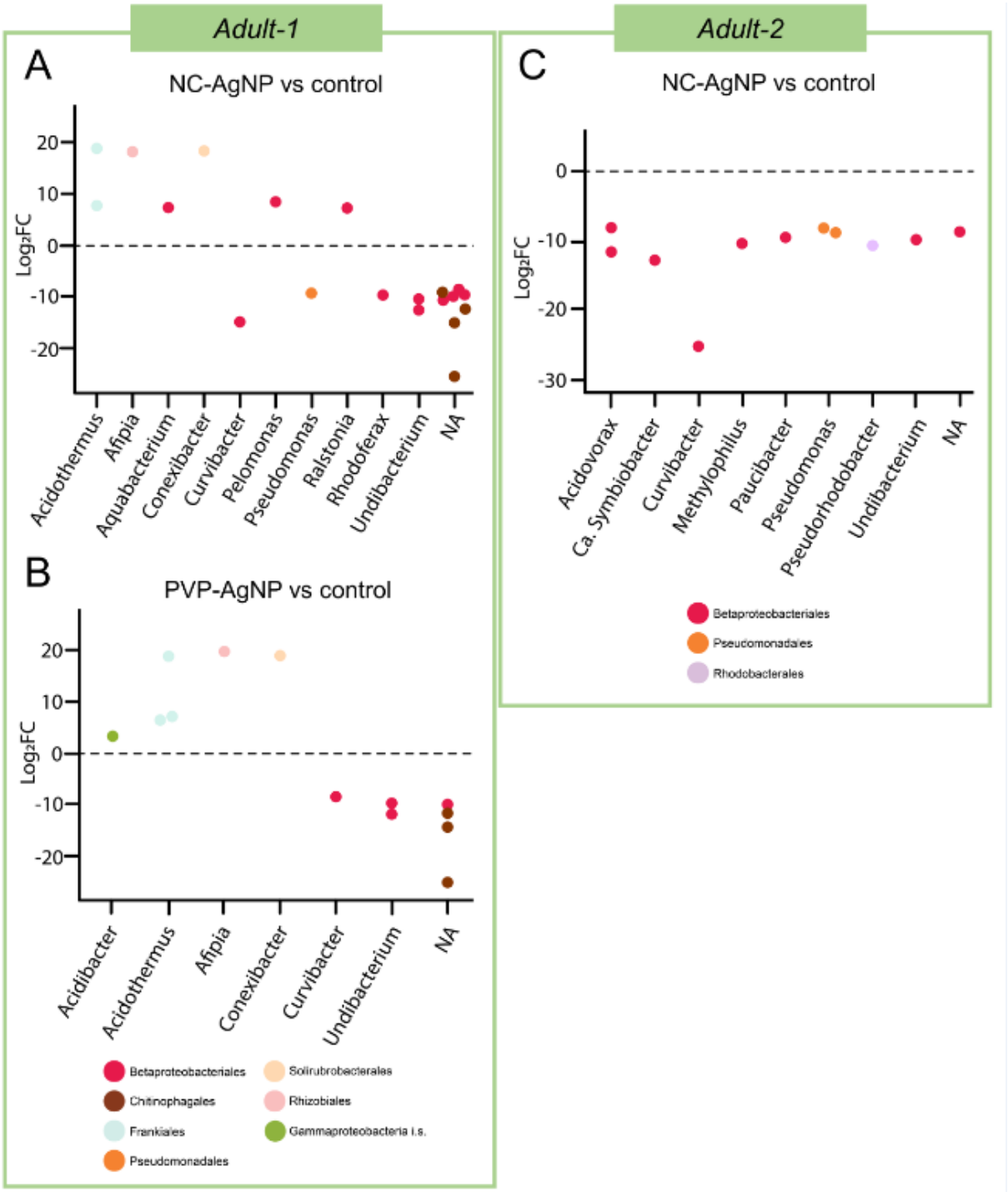

Fig. 3 ASVs that significantly differ in abundance between 7-day AgNP-exposed and non-exposed adult microbiomes (DESeq2, adj-p < 0.05). **A** Comparison between NC-AgNP-exposed and non-exposed microbiomes from the *Adult-1* experiment. (Non-exposed n = 4, NC-AgNP n = 4, PVP-AgNP n = 4) **B** Comparison between PVP-AgNP-exposed and non-exposed microbiomes from experiment *Adult-1*. **C** Comparison between NC-AgNP-exposed and non-exposed microbiomes from experiment *Adult-2*. (Non-exposed n = 4, NC-AgNP n = 4) (NC-AgNPs: non-coated silver nanoparticles, PVP-AgNPs: polyvinylpyrrolidone-coated silver nanoparticles, Log_2FC is defined as Log_2(AgNP/non-exposed), FC: fold change)

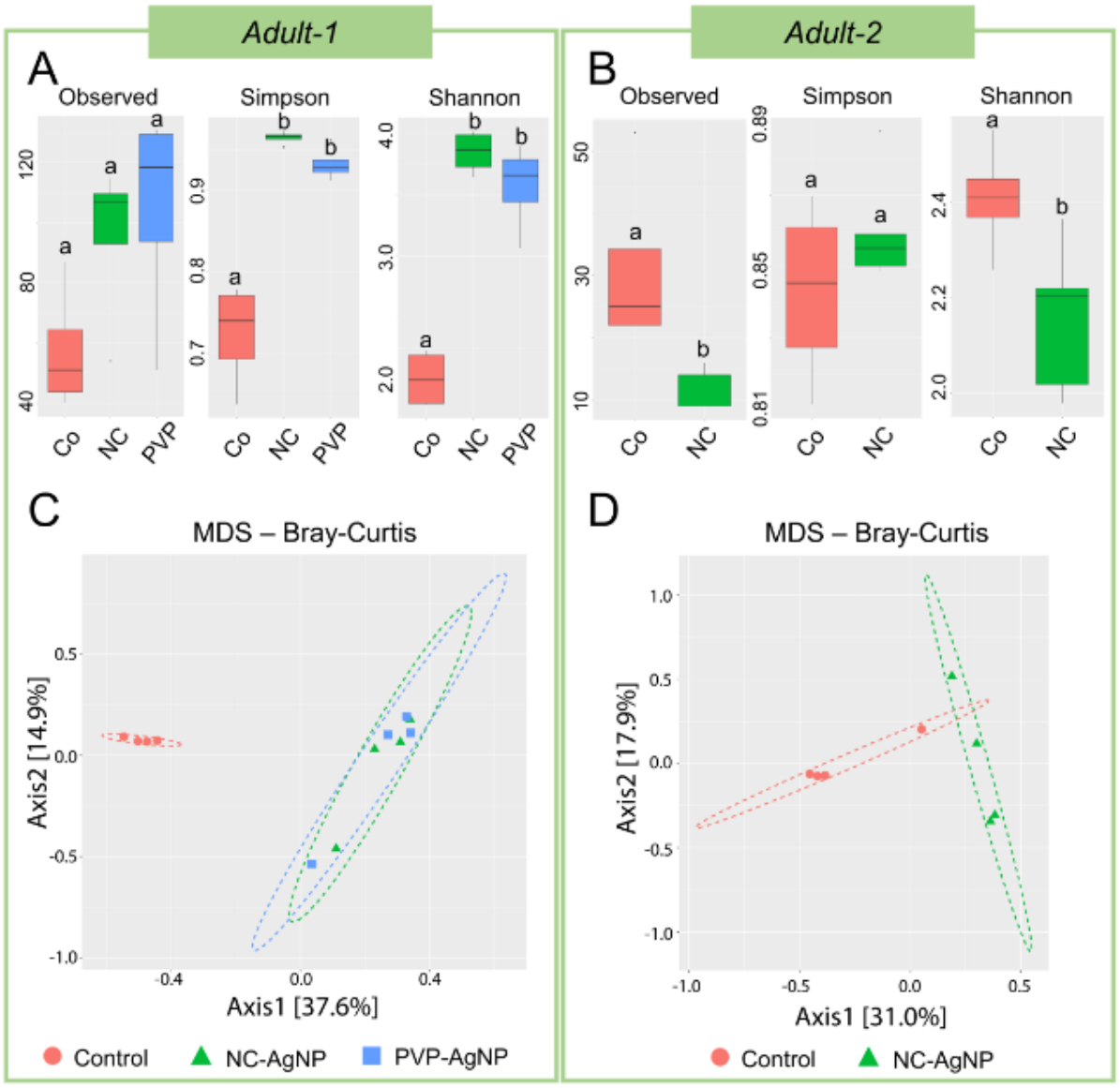

Fig. 4 Alpha- and beta-diversity in the microbiomes of adult worms exposed for 7 days to AgNPs. **A** Alpha-diversity metrics in experiment *Adult-1*: the observed ASV number (ns), Simpson's diversity index ($p = 0.00971$; pairwise: non-exposed vs NC-AgNP: adj-p = 0.043, non-exposed vs PVP-AgNP: adj-p = 0.043, NC-AgNP vs PVP-AgNP: ns) and Shannon's diversity index ($p = 0.0154$; pairwise: non-exposed vs NC-AgNP: adj-p = 0.043, non-exposed vs PVP-AgNP: adj-p = 0.043, NC-AgNP vs PVP-AgNP: ns). (non-exposed n = 4, NC-AgNP n = 4, PVP-AgNP n = 4) **B** Alpha-diversity metrics in experiment *Adult-2*: the observed ASV number ($p = 0.013$), Simpson's diversity index (ns) and Shannon's diversity index ($p = 0.034$). (Non-exposed n = 4, NC-AgNP n = 4) **C** MDS plot based on Bray-Curtis index of dissimilarity on samples of *Adult-1* ($p = 0.005$, $R^2 = 0.456$, perm = 1000; Betadisper: ns; Pairwise: non-exposed vs NC-AgNP: adj-p = 0.044, $R^2 = 0.459$, non-exposed vs PVP-AgNP: adj-p = 0.044, $R^2 = 0.460$, NC-AgNP vs PVP-AgNP: ns, $R^2 = 0.123$). **D** MDS plot based on Bray-Curtis index of dissimilarity on samples of *Adult-2* ($p = 0.030$, $R^2 = 0.280$, perm = 1000; Betadisper: ns). Ellipses are drawn at 85 % confidence interval. (Co: non-exposed, NC/NC-AgNP: non-coated silver nanoparticles, PVP/PVP-AgNP: polyvinylpyrrolidone-coated silver nanoparticles, ns = not significant ($p > 0.05$), the letters on the graphs indicate statistical significance: when letters are different from each other, it means that the corresponding groups differ statistically from each other.)

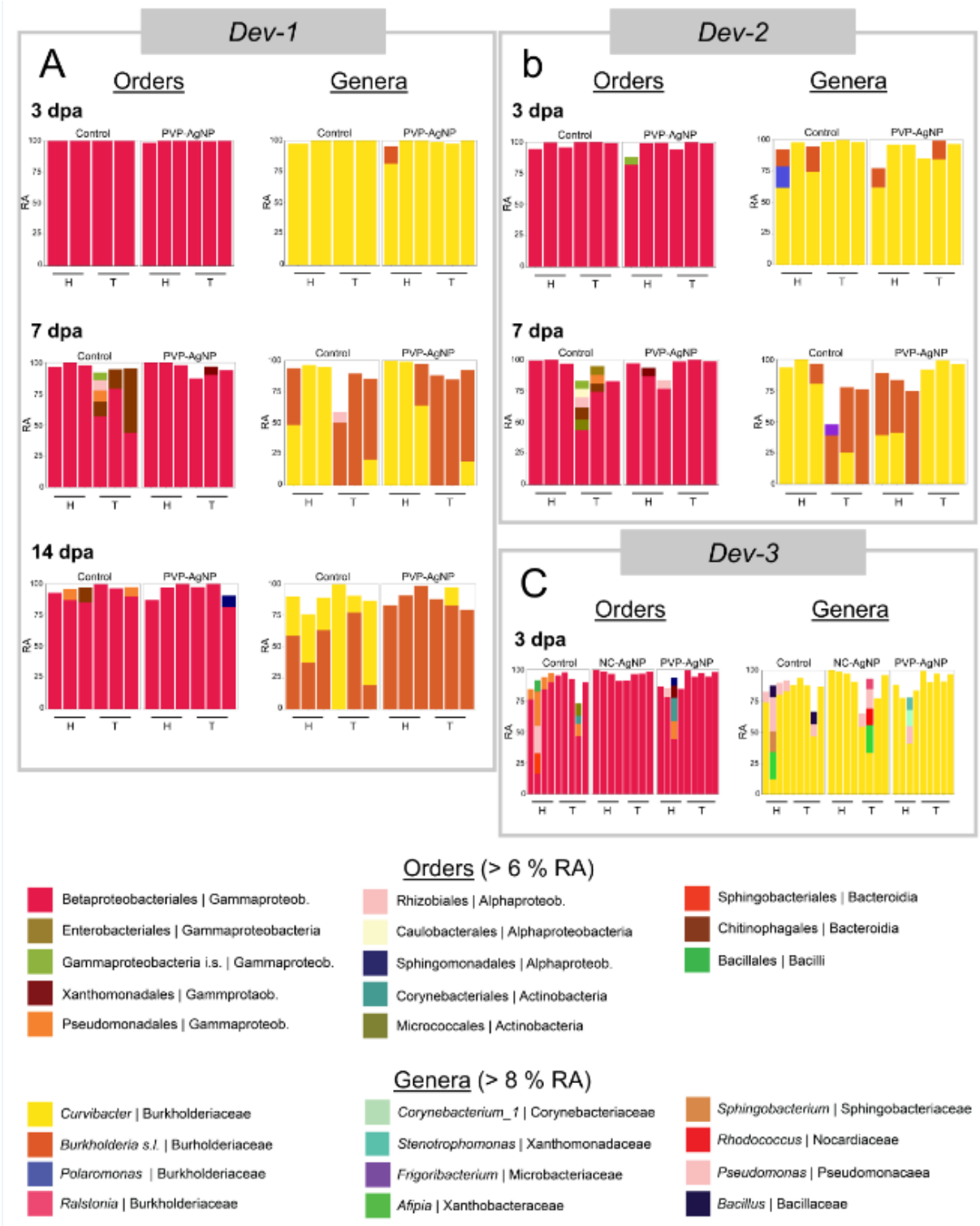

Fig. 5 Relative abundance of taxa in the microbiomes of regenerating worms exposed to AgNPs. **A** RA of bacterial taxa in experiment *Dev-1*, exposed to PVP-AgNP, on order level (> 6% RA) and genus level (> 8% RA), 3, 7 and 14 dpa. (Non-exposed n = 16, PVP-AgNP n = 18) **B** RA of bacterial taxa in experiment *Dev-2*, exposed to PVP-AgNP on order level (> 6% RA) and genus level (> 8% RA), 3 and 7 dpa. (Non-exposed n = 12, PVP-AgNP n = 12) **C** RA of bacterial taxa in experiment *Dev-3*, exposed to NC-AgNP or PVP-AgNP on order level (> 6 % RA) and genus level (> 8% RA), 3 dpa. (Non-exposed n = 9, NC-AgNP n = 8, PVP-AgNP n = 9) (The data in *Dev-1*, *Dev-2* and *Dev-3* represent three independent experiments. NC-AgNP: non-coated silver nanoparticles, PVP-AgNP: polyvinylpyrrolidone-coated silver nanoparticles, i.s.: incertae sedis, s.l.: sensu lato,, H: head, T: tail, RA: relative abundance, dpa: days post amputation. On the right side of the pipe symbol (|), the corresponding higher taxon is indicated.)

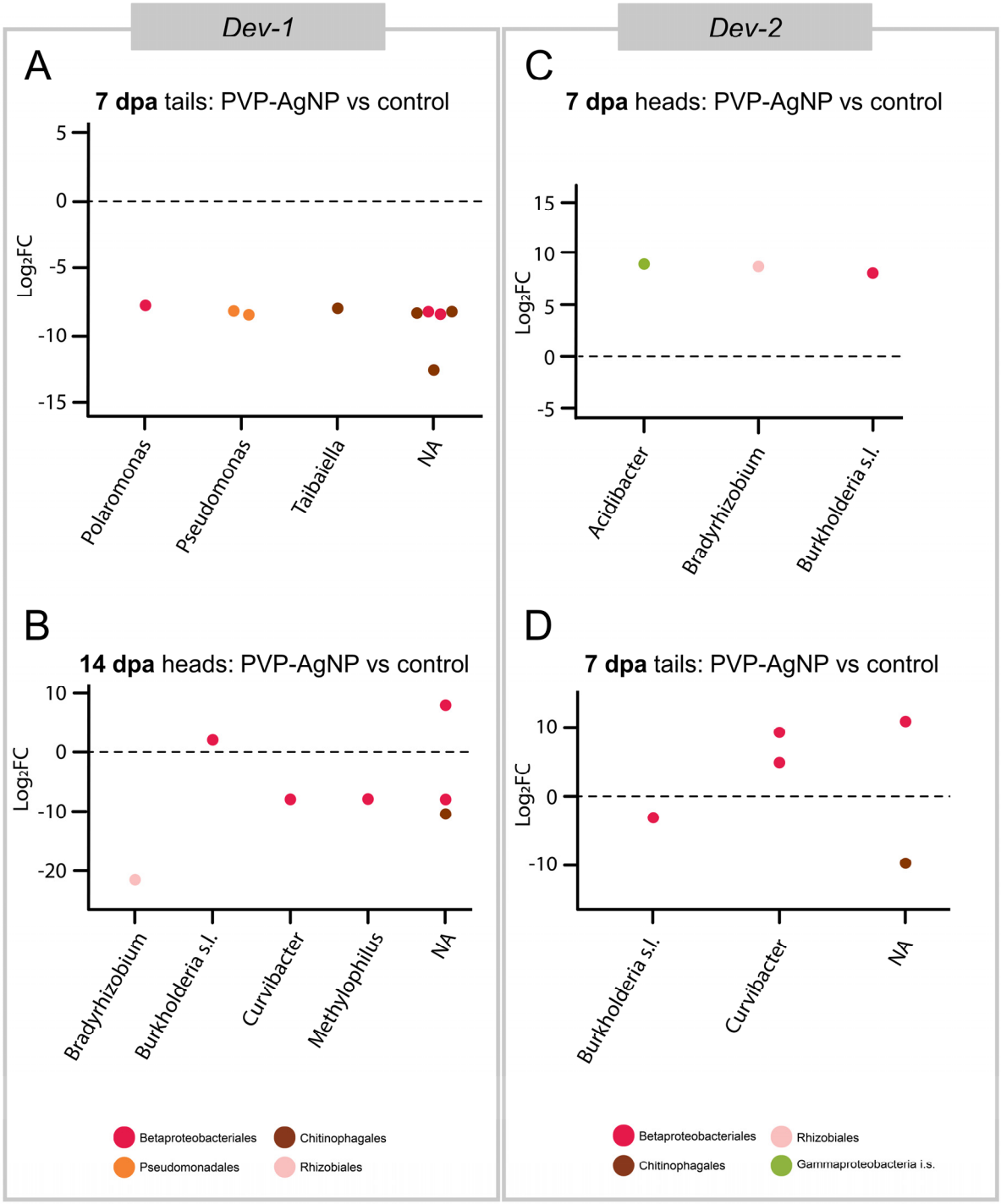

Fig. 6 ASVs that significantly differ in abundance between the microbiomes of PVP-AgNP-exposed and non-exposed regenerating worms (DESeq2, adj-p < 0.05). **A** Comparison between 7 dpa PVP-AgNP-exposed and non-exposed tail microbiomes of the *Dev-1* experiment. (Non-exposed n = 3, PVP-AgNP n = 3) **B** Comparison between 14 dpa PVP-AgNP-exposed and non-exposed head microbiomes of *Dev-1*. **C** Comparison between 7 dpa PVP-AgNP-exposed and non-exposed head microbiomes of *Dev-2*. (Non-exposed n = 3, PVP_AgNP n = 3) **D** Comparison between 7 dpa PVP-AgNP-exposed and non-exposed tail microbiomes of *Dev-2*. (PVP: polyvinylpyrrolidone-coated silver nanoparticles, i.s.: incertae sedis, s.l.: sensu lato, Log_2FC is defined as Log_2(PVP-AgNP/non-exposed), FC: fold change)

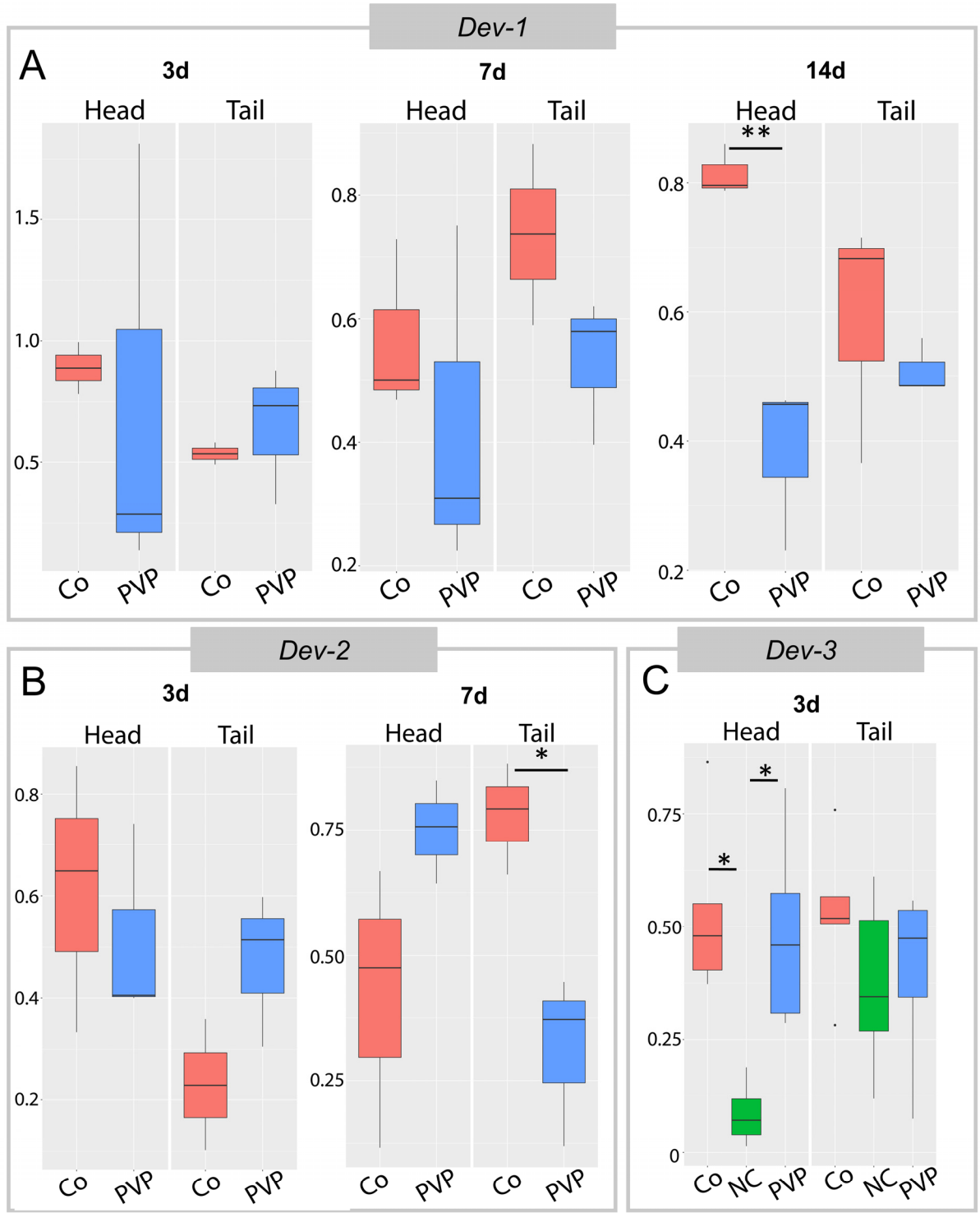

Fig. 7 Alpha-diversity measured by Simpson's diversity index in the microbiomes of regenerating worms exposed to AgNPs. Head and tail fragments were considered separately in the statistical analyses. **A** Comparison between PVP-AgNP-exposed and non-exposed microbiomes in experiment *Dev-1* after day 3 (ns), 7 (ns) and 14 (heads: p = 0.005, tails: ns) of development. (Non-exposed head n = 8, PVP-AgNP head n = 9, Non-exposed tail n = 8, PVP-AgNP tail n = 9) **B** Comparison between PVP-AgNP-exposed and non-exposed microbiomes in experiment *Dev-2* after day 3 (ns) and 7 (heads: ns, tails: p = 0.0167) days of development. (Non-exposed head n = 9, PVP-AgNP head n = 9, non-exposed tail n = 9, PVP-AgNP tail n = 9) **C** Comparison between AgNP-exposed and non-exposed microbiomes in experiment *Dev-3* after 3 days of development. Statistically significant differences in head microbiomes, between non-exposed and NC-AgNP (p = 0.0149) and between PVP-AgNP and NC-AgNP (p = 0.0480). (Non-exposed head n = 4, NC-AgNP head n = 4, PVP-AgNP head n = 4, non-exposed tail n = 5, NC-AgNP tail n = 4, PVP-AgNP tail n = 5) (Co: non-exposed, NC: non-coated silver nanoparticles, PVP: polyvinylpyrrolidone-coated silver nanoparticles, * $p < 0.05$, ** $p < 0.01$, ns: not significant ($p > 0.05$))

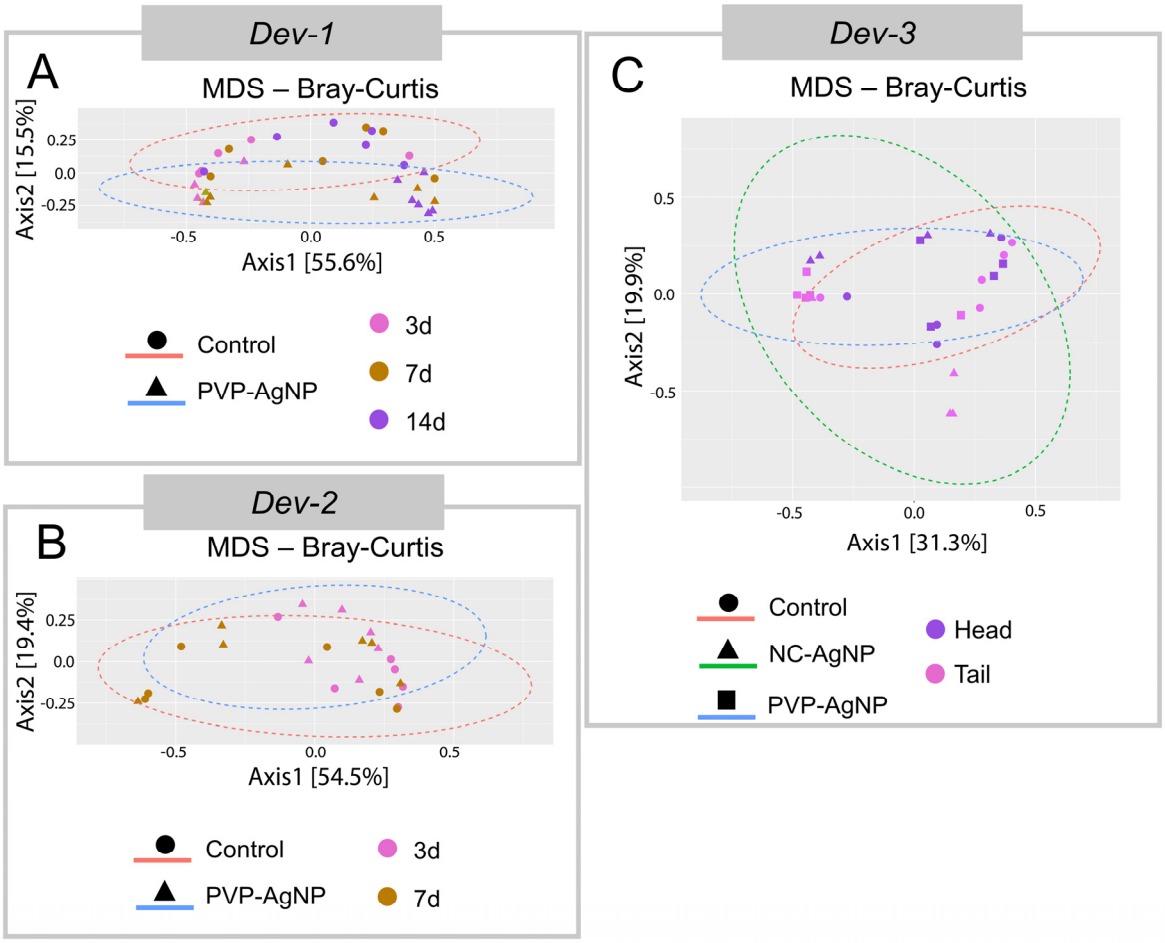

Fig. 8 MDS plot based on Bray-Curtis index of dissimilarity on the microbiomes of regenerating worms exposed to AgNPs. **A** In experiment *Dev-1*, including 3, 7 and 14 dpa head and tail microbiomes: significant effect of exposure ($p = 0.001$, $R^2 = 0.101$), fragment ($p = 0.0340$, $R^2 = 0.041$,) and developmental stage ($p = 0.001$, $R^2 = 0.243$, interaction developmental stage × exposure ($p = 0.0170$, $R^2 = 0.0887$) and interaction fragment × developmental stage ($p = 0.001$, $R^2 = 0.133$). (Non-exposed n = 16, PVP-AgNP n = 18) **B** In experiment *Dev-2*, including 3 and 7 dpa heads and tail microbiomes: significant effect of fragment ($p = 0.004$, $R^2 = 0.128$), interaction fragment × exposure ($p = 0.004$, $R^2 = 0.127$), interaction fragment × developmental stage × exposure ($p = 0.001$, $R^2 = 0.237$). (Non-exposed n = 12, PVP-AgNP n = 12) **C** In experiment *Dev-3*, including 3 dpa heads and tail microbiomes: significant effect of fragment ($p = 0.0210$, $R^2 = 0.0858$), interaction fragment × exposure ($p = 0.002$, $R^2 = 0.188$) (Non-exposed n = 9, NC-AgNP n = 8, PVP-AgNP n = 9) Ellipses are drawn at 85 % confidence interval. (NC-AgNP: non-coated silver nanoparticles, PVP-AgNP: polyvinylpyrrolidone-coated silver nanoparticles)